

This article was downloaded by:

On: 15 January 2011

Access details: *Access Details: Free Access*

Publisher *Taylor & Francis*

Informa Ltd Registered in England and Wales Registered Number: 1072954 Registered office: Mortimer House, 37-41 Mortimer Street, London W1T 3JH, UK



## Comments on Inorganic Chemistry

Publication details, including instructions for authors and subscription information:

<http://www.informaworld.com/smpp/title~content=t713455155>

### **d<sup>0</sup>N-METAL COMPLEXES SUPPORTED BY FERROCENE-BASED CHELATING LIGANDS**

Paula L. Diaconescu<sup>a</sup>

<sup>a</sup> Department of Chemistry and Biochemistry, University of California, Los Angeles, CA, USA

Online publication date: 02 December 2010

**To cite this Article** Diaconescu, Paula L.(2010) 'd<sup>0</sup>N-METAL COMPLEXES SUPPORTED BY FERROCENE-BASED CHELATING LIGANDS', *Comments on Inorganic Chemistry*, 31: 5, 196 – 241

**To link to this Article:** DOI: 10.1080/02603594.2010.534023

**URL:** <http://dx.doi.org/10.1080/02603594.2010.534023>

PLEASE SCROLL DOWN FOR ARTICLE

Full terms and conditions of use: <http://www.informaworld.com/terms-and-conditions-of-access.pdf>

This article may be used for research, teaching and private study purposes. Any substantial or systematic reproduction, re-distribution, re-selling, loan or sub-licensing, systematic supply or distribution in any form to anyone is expressly forbidden.

The publisher does not give any warranty express or implied or make any representation that the contents will be complete or accurate or up to date. The accuracy of any instructions, formulae and drug doses should be independently verified with primary sources. The publisher shall not be liable for any loss, actions, claims, proceedings, demand or costs or damages whatsoever or howsoever caused arising directly or indirectly in connection with or arising out of the use of this material.

---

## **d<sup>0fN</sup>-METAL COMPLEXES SUPPORTED BY FERROCENE-BASED CHELATING LIGANDS**

---

**PAULA L. DIACONESCU**

Department of Chemistry and Biochemistry,  
University of California, Los Angeles, CA, USA

Ferrocene is widely incorporated in pharmaceutical candidates, materials, and redox agents. In addition, ligand scaffolds make use of ferrocene groups because of their steric, electronic, and redox properties. In some cases, ferrocene is involved directly in the reactivity of a metal center even when it is part of the supporting ligand. While metal-ligand cooperation plays an important role in enzymatic catalysis, it is less developed in organometallic chemistry. Our group has focused on ferrocene-based chelating ligands because they possess unique electronic characteristics that make them especially versatile in supporting a wide range of reactivity behaviors for the resulting metal complexes.

The present review discusses the chemistry of metal complexes with two types of ferrocene-based chelating ligands: (1) Schiff base; and (2) diamide. The first class of ligands supports yttrium and cerium alkoxides, while the second class is used for group 3 metal (scandium, yttrium, lutetium, and lanthanum) alkyls.

Two series of Schiff base metal complexes are presented. The two ancillary ligands differ by the type of the N=X functionality that they incorporate: one ligand is based on an imine group, whereas the other is based on an iminophosphorane group. Cerium(IV) bis(alkoxide) complexes were targeted in order to determine whether the presence of a strongly oxidizing metal center would give rise to a non-innocent redox behavior in the supporting ligands. The experimental data indicated that iron remained in the

Address correspondence to Paula L. Diaconescu, Department of Chemistry and Biochemistry, University of California, Los Angeles, CA 90095, USA. E-mail: pld@chem.ucla.edu

+2 oxidation state and that cerium(IV) did not engage any part of the ancillary ligand in redox behavior.

The reactivity of group 3 metal complexes supported by 1,1'-ferrocenylene diamide ligands toward aromatic N-heterocycles is also discussed. These reactions are compared to analogous reactions studied with group 3 metal complexes supported by pincer-type pyridine diamides. That comparison showed that similar reactions were observed with 1-methylimidazole, 2-picoline, and isoquinoline, although other types of reactions and a larger substrate scope were identified for the ferrocene- than for the pyridine-based complexes. Based on the reactions discussed herein and on isolated examples drawn from the literature, it is concluded that the ferrocene diamides represent a versatile and privileged ligand framework. It is proposed that the privileged status of these organometallic ancillary ligands is a consequence of iron's ability to accommodate changes in the electronic density at the metal center more readily than classical supporting ligands.

## 1. INTRODUCTION

The isolation of ferrocene in 1951<sup>[1,2]</sup> represents a major landmark in chemistry. The discovery of its unusual electronic structure<sup>[3-5]</sup> generated so much excitement that it is considered the birth of modern organometallic chemistry.<sup>[6]</sup> This structure is still intensely exploited today and it is incorporated in pharmaceutical candidates, materials, and redox agents.<sup>[7-9]</sup> In addition, ligand scaffolds make use of ferrocene groups because of their steric, electronic, and redox properties. In some cases, ferrocene is involved directly in the reactivity of a metal center even when it is part of the supporting ligand. While metal-ligand cooperation plays an important role in enzymatic catalysis,<sup>[10-13]</sup> it is less developed in organometallic chemistry.<sup>[14]</sup>

Ferrocene-based chelating ligands are particularly interesting because they impart special steric and electronic properties to the resulting metal complexes. In this class, 1,1'-bis(diphenylphosphine)ferrocene (dppf)<sup>[15,16]</sup> is probably the most well known example because of its applications to organic catalysis.<sup>[8]</sup> In the quest of developing alternatives to metallocene  $\alpha$ -olefin polymerization catalysts,<sup>[17]</sup> chelating diamides have emerged as great supporting ligands for early transition metals.<sup>[18]</sup> Such endeavors have provided an important stimulus for the synthesis of 1,1'-di(heteroatom)-functionalized ferrocenes, where the heteroatom is nitrogen, oxygen, and sulfur.<sup>[19]</sup>

We embarked on a road to uncover new bonding motifs and reactivity of metal complexes as a result of supporting ligand design.  $d^0f^n$ -Metal complexes were targeted because they incorporate highly electrophilic metal centers that prove advantageous in reactions with relatively unreactive substrates.

## 2. ALKOXIDE COMPLEXES SUPPORTED BY IMINE-BASED LIGANDS

The lanthanides offer the possibility to study the interaction between ferrocene ligands and redox-active and inactive metals. Only one lanthanide, cerium(IV), is known to act as an oxidizing agent. A strongly oxidizing metal center may transform the ferrocene in the backbone of a supporting ligand into ferrocenium upon coordination. Cerium(IV) has a redox potential of 0.88 V in water, while iron(III) has a redox potential of 0.00 V (both referenced versus  $\text{Cp}_2\text{Fe}/\text{Cp}_2\text{Fe}^+$ ).<sup>[9]</sup> Therefore, cerium(IV) alkoxides supported by Schiff bases incorporating ferrocene (Chart 1)<sup>[20]</sup> were targeted in order to determine whether cerium(IV) could oxidize the ferrocene backbone or a different functionality of the ancillary ligand.<sup>[21]</sup> Schiff bases incorporating ferrocene, such as 1,1'-di(2,4-bis-*tert*-butyl-salicylimino)ferrocene ( $\text{H}_2(\text{NN}^{\text{sal}})$ ), had been previously used to generate magnesium, titanium, and zirconium complexes; however, the redox properties of those complexes were not investigated.<sup>[22]</sup> A new ferrocene diphosphazene proligand, 1,1'-di(2-*tert*-butyl-6-diphenylphosphiminophenol)ferrocene ( $\text{H}_2(\text{NN}^{\text{phos}})$ ), and its complexes (Chart 1) were also synthesized and characterized to study

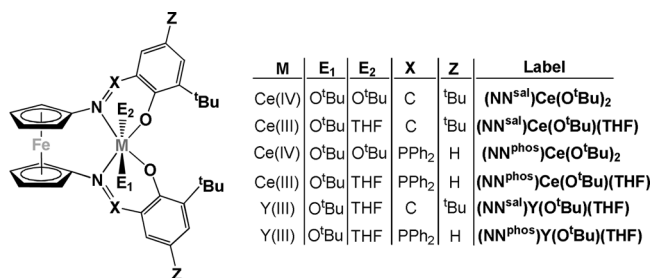


Chart 1. Schiff base ferrocene cerium and yttrium alkoxide complexes.

whether the imine bond is important in determining the electronic properties of the resulting compounds.

It is important to note that although the structures of Schiff base metal complexes have been thoroughly studied,<sup>[23]</sup> complexes of  $d^{0f^n}$  metals had not been the subject of electrochemical investigations. Several studies of the electrochemical properties of Schiff base metal complexes were reported<sup>[24,25]</sup> and, in certain cases, ligand-based oxidations were identified.<sup>[26–36]</sup>

Both cerium(IV) complexes were synthesized from  $\text{Ce}(\text{O}^t\text{Bu})_4 \cdot (\text{THF})_2$  and the protonated pro-ligands. For cerium(III) and yttrium(III) alkoxide complexes, two methods were used: (1) the reaction of the  $\text{M}[\text{N}(\text{SiMe}_3)_2]_3$  ( $\text{M} = \text{Ce}$ ) with the protonated pro-ligands ( $\text{H}_2(\text{NN}^{\text{sal}})$ ), followed by the reaction with *t*-butanol; and (2) salt metathesis between the metal trichloride and the disodium salts of the pro-ligands to give the monochloride complexes, which, in turn, reacted with potassium *tert*-butoxide to form the corresponding alkoxides.<sup>[21]</sup> All the metal complexes were characterized by cyclic voltammetry and  $^1\text{H}$  NMR, Mössbauer, X-ray absorption near-edge structure (XANES), and absorption spectroscopies. In addition,  $(\text{NN}^{\text{sal}})\text{Ce}(\text{O}^t\text{Bu})_2$  and  $(\text{NN}^{\text{phos}})\text{Ce}(\text{O}^t\text{Bu})_2$  (Figure 1) were characterized by single-crystal X-ray crystallography. Both complexes contain a pseudo-octahedral cerium ion, with the two *t*-butoxide ligands coordinated trans in the axial positions. Metrical parameters for the coordination environment of cerium are

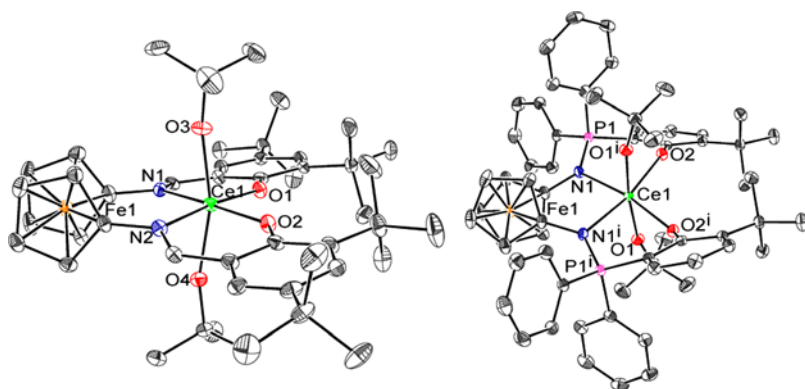
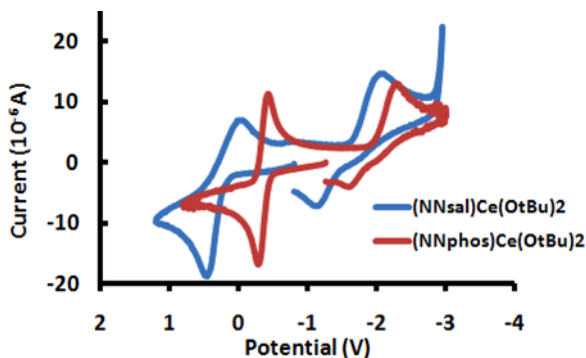


Figure 1. ORTEP representations (thermal ellipsoids at 50% probability) of  $(\text{NN}^{\text{sal}})\text{Ce}(\text{O}^t\text{Bu})_2$  (left) and  $(\text{NN}^{\text{phos}})\text{Ce}(\text{O}^t\text{Bu})_2$  (right); hydrogen atoms were removed for clarity. (Figure appears in color online.)



**Figure 2.** Cyclic voltammograms of  $(\text{NN}^{\text{sal}})\text{Ce}(\text{O}^t\text{Bu})_2$  and  $(\text{NN}^{\text{phos}})\text{Ce}(\text{O}^t\text{Bu})_2$  at 100 mV/s scan rate (1.5 mM in THF, 0.5 M  $[\text{Pr}_4\text{N}][\text{BAR}_4^{\text{F}}]$ ,  $\text{Cp}_2\text{Fe}/\text{Cp}_2\text{Fe}^+$  corrected). (Figure appears in color online.)

similar for the two complexes, except that there is a larger deviation from the planarity of the  $\text{NCeO}_{\text{phenoxide}}$  arrangements in  $(\text{NN}^{\text{phos}})\text{Ce}(\text{O}^t\text{Bu})_2$  than in  $(\text{NN}^{\text{sal}})\text{Ce}(\text{O}^t\text{Bu})_2$ .<sup>[21]</sup>

Cyclic-voltammetry studies were undertaken to probe the redox events feasible to occur within the cerium(IV) alkoxide complexes (Figure 2 and Table 1). The cyclic voltammograms of the two pro-ligands  $\text{H}_2(\text{NN}^{\text{sal}})$  and  $\text{H}_2(\text{NN}^{\text{phos}})$  show one redox event that was assigned to the  $\text{Fe}^{2+/3+}$  couple. Changing the imine with a phosphorimine functionality resulted in a more reducing potential for the  $\text{Fe}^{2+/3+}$  event in  $\text{H}_2(\text{NN}^{\text{phos}})$  ( $-0.633$  V) than in  $\text{H}_2(\text{NN}^{\text{sal}})$  ( $0.287$  V). All metal complexes show a

**Table 1.** Redox events for the compounds discussed<sup>a</sup>

Complex	$E_{1/2}(\text{Fe}^{2+/3+})$ (V)	$E_{1/2}(\text{Ce}^{3+/4+})$ (V)
$\text{H}_2(\text{NN}^{\text{sal}})$	$0.29^b$	—
$\text{H}_2(\text{NN}^{\text{phos}})$	$-0.63^c$	—
$(\text{NN}^{\text{sal}})\text{Y}(\text{O}^t\text{Bu})(\text{THF})$	$0.09^c$	—
$(\text{NN}^{\text{phos}})\text{Y}(\text{O}^t\text{Bu})(\text{THF})$	$-0.29^b$	—
$(\text{NN}^{\text{sal}})\text{Ce}(\text{O}^t\text{Bu})(\text{THF})$	$E_{\text{ox}} = -0.21^c$ $E_{\text{red}} = -1.05$	—
$(\text{NN}^{\text{phos}})\text{Ce}(\text{O}^t\text{Bu})(\text{THF})$	$-0.57^b$	—
$(\text{NN}^{\text{sal}})\text{Ce}(\text{O}^t\text{Bu})_2$	$-0.28^b$	$E_{\text{ox}} = -1.01^b$ $E_{\text{red}} = -2.07$
$(\text{NN}^{\text{phos}})\text{Ce}(\text{O}^t\text{Bu})_2$	$-0.38^b$	$E_{\text{ox}} = -1.70^b$ $E_{\text{red}} = -2.39$

<sup>a</sup>Numbers are from 250 mV/s scans.

<sup>b</sup>1.5 mM in THF, 0.5 M  $[\text{Pr}_4\text{N}][\text{BAR}_4^{\text{F}}]$ ,  $\text{Cp}_2\text{Fe}/\text{Cp}_2\text{Fe}^+$  corrected.

<sup>c</sup>2.0 mM in THF, 0.5 M  $[\text{Pr}_4\text{N}][\text{BAR}_4^{\text{F}}]$ ,  $\text{Cp}_2\text{Fe}/\text{Cp}_2\text{Fe}^+$  corrected.

reversible (quasi-reversible for  $(\text{NN}^{\text{sal}})\text{Ce}(\text{O}^t\text{Bu})(\text{THF})$ ), one-electron event that was assigned to the  $\text{Fe}^{2+/3+}$  couple. In addition, the cerium(IV) complexes,  $(\text{NN}^{\text{sal}})\text{Ce}(\text{O}^t\text{Bu})_2$  and  $(\text{NN}^{\text{phos}})\text{Ce}(\text{O}^t\text{Bu})_2$ , show an irreversible reduction/oxidation event that was assigned to the  $\text{Ce}^{4+/3+}$  couple (Figure 2). The oxidation of cerium in  $(\text{NN}^{\text{sal}})\text{Ce}(\text{O}^t\text{Bu})(\text{THF})$  and  $(\text{NN}^{\text{sal}})\text{Ce}(\text{O}^t\text{Bu})(\text{THF})$  was not observed. Overall, it was easier to oxidize the backbone of the iminophosphorane than of the imine complexes and it was more difficult to reduce cerium(IV) to cerium(III) in  $(\text{NN}^{\text{phos}})\text{Ce}(\text{O}^t\text{Bu})_2$  than in  $(\text{NN}^{\text{sal}})\text{Ce}(\text{O}^t\text{Bu})_2$ .<sup>[21]</sup>

All other experimental data indicated that iron remains in the +2 oxidation state and that cerium(IV) did not engage any part of the ancillary ligand in redox behavior.

The cerium(IV) complexes supported by  $\text{NN}^{\text{sal}}$  were used as the first cerium(IV) alkoxide catalysts for the ring-opening polymerization of lactide.<sup>[20]</sup> Although rare earth alkoxides had been studied extensively as catalysts for the ring-opening polymerization (ROP) of cyclic esters,<sup>[37–40]</sup> cerium(IV) examples were virtually unknown.<sup>[41]</sup> The lactide polymerization activity of  $(\text{NN}^{\text{sal}})\text{Ce}(\text{O}^t\text{Bu})_2$  was compared to the activity of  $(\text{NN}^{\text{sal}})\text{Y}(\text{O}^t\text{Bu})(\text{THF})$  and to that of  $\text{Ce}(\text{O}^t\text{Bu})_4(\text{THF})_2$ . The complex  $(\text{NN}^{\text{sal}})\text{Ce}(\text{O}^t\text{Bu})_2$  was less active than  $\text{Ce}(\text{O}^t\text{Bu})_4(\text{THF})_2$  and  $(\text{NN}^{\text{sal}})\text{Y}(\text{O}^t\text{Bu})(\text{THF})$  (Table 2). It was found, however, from reactions with D,L-lactide, that the ancillary ligand bound to the metal center prevented chain transfer.

The different activities of the cerium(IV) and yttrium(III)  $\text{NN}^{\text{sal}}$  complexes were explained on the basis of the electrophilicity of the metal center. Investigation of Mulliken charges for the corresponding model complexes showed that yttrium had a higher charge (1.92) than cerium (IV) (1.64) in the respective complexes. The same trend was observed for the *t*-butoxide oxygen charges:  $-0.87$  for the yttrium and  $-0.66$  (average value) for the cerium  $\text{NN}^{\text{sal}}$  model complex.

### 3. ALKYL COMPLEXES SUPPORTED BY DIAMIDE LIGANDS

1,1'-Ferrocenylene diamides ( $\text{NN}^{\text{fc}}$ , Chart 2) appeared to be desirable supporting frameworks because of a number of characteristics:

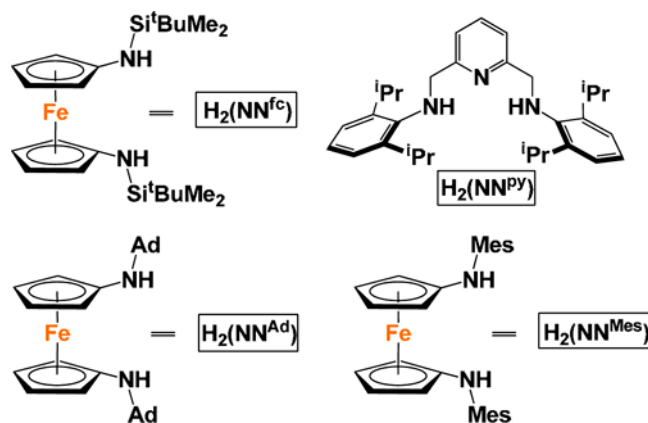
1. They are chelating ligands and, by enforcing a *cis*-coordination of the two amide donors, block one side of the  $d^0f^n$  metal center, leaving the other side open to attack by various substrates.

**Table 2.** Data for ROP of lactide by  $(\text{NN}^{\text{sal}})\text{Ce}(\text{O}^t\text{Bu})_2$  ( $70^\circ\text{C}$ ),  $\text{Ce}(\text{O}^t\text{Bu})_4(\text{THF})_2$  and  $(\text{NN}^{\text{sal}})\text{Y}(\text{O}^t\text{Bu})(\text{THF})$  (room temperature)

Catalyst	eq LA	Time (min)	Conversion (%)	$M_n$ (kg/mol) <sup>a</sup>	PDI
$(\text{NN}^{\text{sal}})\text{Ce}(\text{O}^t\text{Bu})_2$	100	20	94	32.7	1.45
	200	20	90	53.4	1.36
	300	35	89	58.4	1.39
	400	35	94	47.4	1.55
	500	48	88	64.7	1.27
$\text{Ce}(\text{O}^t\text{Bu})_4(\text{THF})_2$	100	20	96	5.8	1.54
	200	20	89	13.5	1.34
	300	20	92	24.8	1.67
	400	40	82	23.7	1.15
	500	40	98	17.5	1.24
$(\text{NN}^{\text{sal}})\text{Y}(\text{O}^t\text{Bu})(\text{THF})$	100	5	97	17.9	1.21
	200	5	98	42.1	1.15
	300	15	98	59.1	1.19
	400	40	86	66.3	1.17
	500	40	90	92.9	1.13

<sup>a</sup>Molecular weights ( $M_n$ ) were corrected by a Mark-Houwink factor of 0.58 (PS standards were used).

2. The ferrocene backbone has the ability to accommodate changes in the electronic density at the  $d^0$ -metal center by varying the geometry around iron.

**Chart 2.** Diamine pro-ligands discussed. (Chart appears in color online.)



3. A weak interaction of donor-acceptor type may occur between iron and the  $d^0f^n$  metal, possibly influencing the reactivity of the complex.
4. The ligand backbone is redox active.

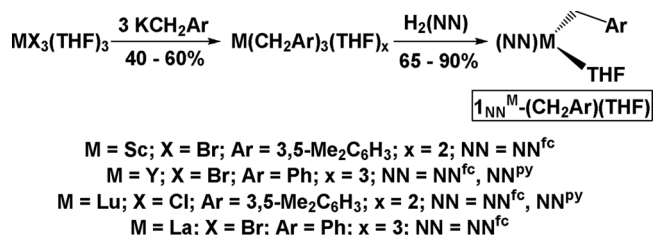
The first feature proved important in stabilizing mononuclear complexes and allowing reactions with bulky substrates. A combination of characteristics (1) and (3) gives these ligands a close resemblance to pincer ligands; therefore, we also prepared the analogous complexes of 2,6-bis(2,6-diisopropylanilidomethyl)pyridine ( $NN^{py}$ , Chart 2) for comparison. The unique characteristics of the ferrocene-based ligands, however, are likely responsible for the plethora of new complexes and reaction outcomes observed.

Ferrocene-diamide complexes were initially reported for group 4 metals by Arnold et al.,<sup>[42–44]</sup> who also showed that a highly reactive, cationic titanium(IV) species was stabilized by an interaction with the iron center.<sup>[45]</sup> Such interactions had been proposed earlier for late transition metals.<sup>[46]</sup> Recently, the Stephan group has reported that ferrocenyl can stabilize cyclopentadienyl group 4 metal alkyl cations through an iron-metal interaction.<sup>[47]</sup> Since we started our work with  $NN^{fc}$ , other groups have reported complexes of group 3 metals supported by 1,1'-ferrocene diamides.<sup>[48,49]</sup> Some of our work with  $d^0f^n$ -metal alkyl complexes has been recently reviewed<sup>[50]</sup>; therefore, the present review is organized based on a reaction, instead of a substrate type.

### 3.1. SYNTHESIS AND CHARACTERIZATION OF ALKYL COMPLEXES

Group 3 metal benzyl complexes were synthesized by acid-base reactions from the corresponding *tris*(benzyl) compounds and the pro-ligands  $H_2(NN^{fc})$  ( $NN^{fc} = fc(NSi^tBuMe_2)_2$ ,  $fc = 1,1'$ -ferrocenylene) or  $H_2(NN^{py})$  to give  $1_{fc}^M-(CH_2Ar)(THF)$  (Scheme 1;  $M = Sc, Lu$ :  $Ar = 3,5-Me_2C_6H_3$ ;  $M = Y$ ,  $La$ :  $Ar = Ph$ )<sup>[51–54]</sup> or  $1_{py}^M-(CH_2Ar)(THF)$  (Scheme 1;  $M = Y$ ,  $Ar = Ph$ ;  $M = Lu$ ,  $Ar = 3,5-Me_2C_6H_3$ ),<sup>[55]</sup> respectively.

The solid-state structures of all  $1_{fc}^M-(CH_2Ar)(THF)$  complexes were determined by single-crystal X-ray diffraction (Table 3). For scandium, yttrium, and lutetium, the iron-metal distance is larger than the sum of the covalent radii<sup>[56]</sup> (entries 1–5), while for lanthanum it is smaller (entry 7). This distance is responsive to the electronic make-up of the



**Scheme 1.** Syntheses of group 3 metal benzyl complexes supported by ferrocene- and pyridine-diamide ligands.

ancillary ligand, as shown by the substitution of the silyl by an adamantyl group in  $[\text{fc}(\text{NAd})_2]\text{Lu}(\text{CH}_2\text{Ar})(\text{DME})$  ( $1_{\text{Ad}}^{\text{Lu}} - (\text{CH}_2\text{Ar})(\text{DME})$ , Ad = 2-adamantyl),<sup>[57]</sup> causing it to increase (entry 5), or by a mesityl group in  $[\text{fc}(\text{NMes})_2]\text{Lu}(\text{CH}_2\text{Ar})(\text{THF})$  ( $1_{\text{Mes}}^{\text{Lu}} - (\text{CH}_2\text{Ar})(\text{THF})$ , Mes = 2,4,6-Me<sub>3</sub>C<sub>6</sub>H<sub>2</sub>),<sup>[50]</sup> causing it to decrease (entry 6). The presence of two instead of one ether donors also causes the iron-metal distance to increase (entries 1–2 and 4–5).

DFT calculations were employed to probe the iron–metal interaction.<sup>[50]</sup> Nalewajski-Mrozek bond orders for the metal-iron interaction have relatively small values (Table 4). It is interesting to point out that these values are similar to those calculated for the bond between the group 3 metal and the ether-oxygen donor (ca. 0.2). The calculated bond order for the metal-iron interaction varies only slightly with the nature of the metal center in benzyl complexes (entries 1, 3, 4, and 7). For the same metal center, the bond order is dependent on the nature of the ligands present: the more electron-donating the ligands, the

**Table 3.** Comparison of iron-metal distances in d<sup>0</sup>m-metal alkyl complexes

Entry	Complex	X-ray Fe-M distance (Å)	Sum of covalent radii (Å)	Δ <sub>Fe-M</sub> (Å)	Reference
1	$1_{\text{fc}}^{\text{Sc}} - (\text{CH}_2\text{Ar})(\text{THF})$	3.16	3.02	+0.14	51
2	$1_{\text{fc}}^{\text{Sc}} - (\text{Me})(\text{THF})_2$	3.26	3.02	+0.24	51
3	$1_{\text{fc}}^{\text{Y}} - (\text{CH}_2\text{Ph})(\text{THF})$	3.24	3.22	+0.02	52
4	$1_{\text{fc}}^{\text{Lu}} - (\text{CH}_2\text{Ar})(\text{THF})$	3.25	3.19	+0.06	53
5	$1_{\text{Ad}}^{\text{Lu}} - (\text{CH}_2\text{Ar})(\text{DME})$	3.34	3.19	+0.15	57
6	$1_{\text{Mes}}^{\text{Lu}} - (\text{CH}_2\text{Ar})(\text{THF})$	3.12	3.19	−0.07	50
7	$1_{\text{fc}}^{\text{La}} - (\text{CH}_2\text{Ar})(\text{THF})$	3.38	3.39	−0.01	54

**Table 4.** DFT calculated parameters for  $d^{0n}$ -metal alkyl complexes

Entry	Complex	Calculated Fe-M (X-ray) distance (Å)	Fe-M bond order <sup>a</sup>	Bader charge of M	Bader charge of C <sub>Bz</sub>
1	1 <sup>Sc</sup> <sub>fc</sub> -(CH <sub>2</sub> Ar)(THF)	3.18 (3.16)	0.27	1.83	−0.39
2	1 <sup>Sc</sup> <sub>fc</sub> -Me(THF) <sub>2</sub>	3.38 (3.26)	0.14	—	—
3	1 <sup>Y</sup> <sub>fc</sub> -(CH <sub>2</sub> Ph)(THF)	3.33 (3.24)	0.24	1.95	−0.35
4	1 <sup>Lu</sup> <sub>fc</sub> -(CH <sub>2</sub> Ar)(THF)	3.32 (3.25)	0.22	1.92	−0.37
5	1 <sup>Lu</sup> <sub>Ad</sub> -(CH <sub>2</sub> Ar)(DME)	3.36 (3.34)	0.16	1.96	−0.39
6	1 <sup>Lu</sup> <sub>Mes</sub> -(CH <sub>2</sub> Ar)(THF)	3.36 (3.12)	0.19	1.90	−0.40
7	1 <sup>La</sup> <sub>fc</sub> -(CH <sub>2</sub> Ar)(THF)	3.41 (3.38)	0.27	1.97	−0.31

<sup>a</sup>Nalewajski-Mrozek bond orders.

weaker the metal-iron interaction. This effect is seen when modifying the non-ferrocene ligands (entries 1 and 2) or when changing the electronic properties of the nitrogen donor (entries 4, 5).

Although the trend observed with metal Bader charges needs to be verified by experimental data, it is interesting to note that these values increase in the order: Sc < Lu < Y < La, which is the inverse order expected based on their Lewis acidities.<sup>[58]</sup> These differences are small and because geometry optimizations of key structures did not yield a good agreement with the experimental metal-iron distances, a rigorous interpretation of the variation in calculated charges is not attempted here. For the same series of benzyl complexes, the charge on the benzyl carbon atom is almost unchanged.

Molecular orbitals are shown in Figure 3 for 1<sup>Sc</sup><sub>fc</sub>-(CH<sub>2</sub>Ar)(THF) and 1<sup>Sc</sup><sub>fc</sub>-(Me)(THF)<sub>2</sub>. In agreement with the bond order calculations, the molecular orbitals for 1<sup>Sc</sup><sub>fc</sub>-(CH<sub>2</sub>Ar)(THF) show a stronger iron-scandium interaction than for 1<sup>Sc</sup><sub>fc</sub>-(Me)(THF)<sub>2</sub>. While both HOMO and HOMO-3 show an overlap between scandium and iron atomic orbitals for 1<sup>Sc</sup><sub>fc</sub>-(CH<sub>2</sub>Ar)(THF), the HOMO (or other frontier orbitals) of 1<sup>Sc</sup><sub>fc</sub>-(Me)(THF)<sub>2</sub> is mainly ferrocene based, with almost no contribution from scandium.

From a geometrical point of view, 1,1'-ferrocenylenylene diamides resemble pincer diamides. DFT calculations carried out on full structures for pyridine-diamide yttrium and lutetium benzyl complexes show that the Bader charges (2.00 for Y, 1.95 for Lu) are comparable to the analogous values in the ferrocene-diamide complexes (Table 4).

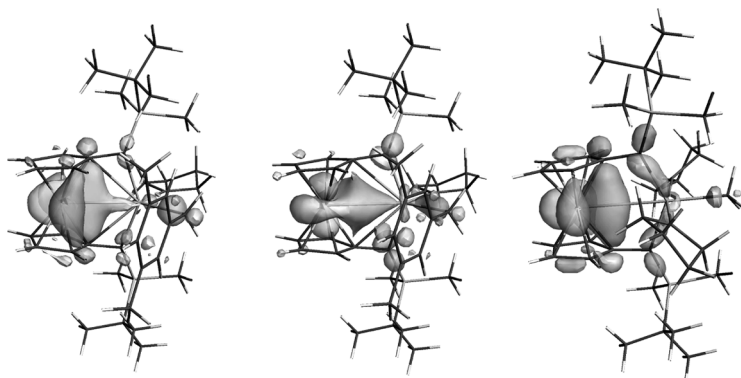


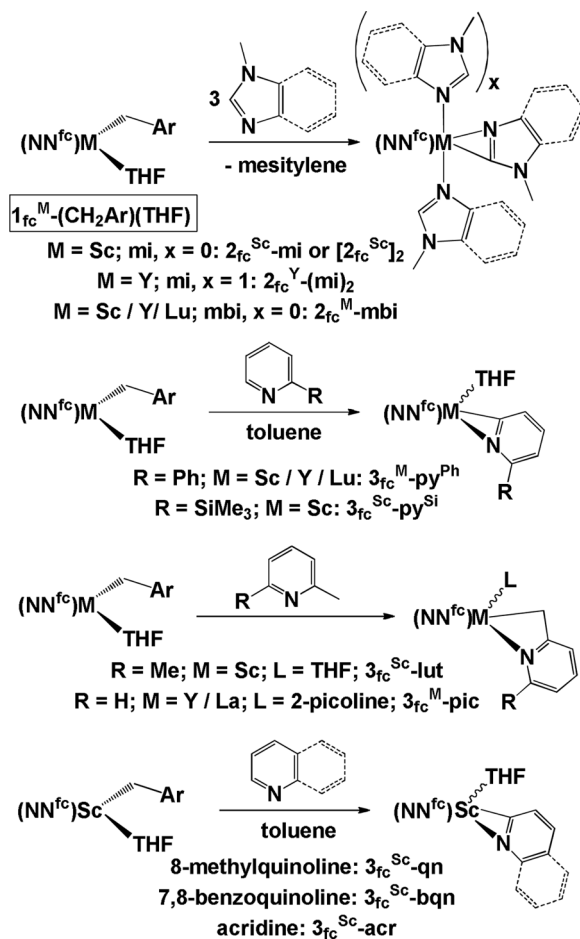
Figure 3. Frontier molecular orbitals for  $1^{\text{Sc}}_{\text{fc}}\text{-(CH}_2\text{Ar)(THF)}$  (left, HOMO; middle, HOMO-3) and  $1^{\text{Sc}}_{\text{fc}}\text{-(Me)(THF)}_2$  (right, HOMO).

### 3.2. Reactions with Aromatic N-Heterocycles

The Bader charges calculated for M in  $1^{\text{M}}_{\text{fc}}\text{-(CH}_2\text{Ar)(THF)}$  (Table 4) are similar to those found for  $\text{Cp}^*_2\text{M(CH}_2\text{Ph)}$  (M = Sc, 1.74). Although the metal centers are highly electrophilic, all group 3 metal benzyl complexes coordinate THF. In order to compare their reactivity to that of the analogous metallocenes, reactions with aromatic N-heterocycles, which can displace the coordinated THF, were studied. Since  $[\text{Cp}^*_2\text{ZrMe(THF)}]^+$  did not C–H activate 1-methylimidazole (only coordination was observed),<sup>[59]</sup> the reactions of this substrate toward the group 3 metal alkyl complexes were tested first.

**3.2.1. C–H Activation.** The C–H activation of aromatic N-heterocycles is a complimentary process to the metalation reactions with main-group organometallic reagents.<sup>[60]</sup> The ortho-metalated products of the reactions between 1-methylimidazoles or pyridines and group 3 metal alkyl complexes, a result of  $\sigma$ -bond metathesis,<sup>[61–63]</sup> were characterized for the ferrocene diamide  $\text{NN}^{\text{fc}}$  (Scheme 2). For the other diamide ligands, it is likely that analogous products form, but they were not isolated.

For 1-methylimidazole (mi), the first step of the reaction involves displacement of THF and coordination of two imidazole molecules. The C–H activation of one of the 1-methylimidazole ligands to give  $2^{\text{M}}_{\text{fc}}\text{-(mi)}_x$  ( $x = 1$  for Sc and 2 for Y) is a relatively slow process. This is



Scheme 2. C–H activation reactions with the group 3 metal benzyl complexes  $1_{\text{fc}}^{\text{M}}\text{-(CH}_2\text{Ar)(THF)}$ .

consistent with the fact that  $[\text{Cp}_2\text{ZrMe(THF)}]^+$  did not promote the C–H activation of 1-methylimidazole.<sup>[59]</sup> All attempts to isolate a THF or non-chelating pyridine solvate of  $(\text{NN}^{\text{fc}})\text{Sc}(\eta^2\text{-N,C-imidazolyl})$  resulted in the formation of  $[(\text{NN}^{\text{fc}})\text{Sc}(\mu^2, \kappa^2\text{-N,C-2-(1-methylimidazolyl)})_2]$ ,  $[2_{\text{fc}}^{\text{Sc}}]_2$ ,<sup>[64]</sup> in which the two scandium centers are bridged by two imidazolyl ligands. The complexes  $2_{\text{fc}}^{\text{Y}}\text{-(mi)}_2$  and  $[2_{\text{fc}}^{\text{Sc}}]_2$  were crystallographically characterized (Figure 4). The complex  $[2_{\text{fc}}^{\text{Sc}}]_2$  features a

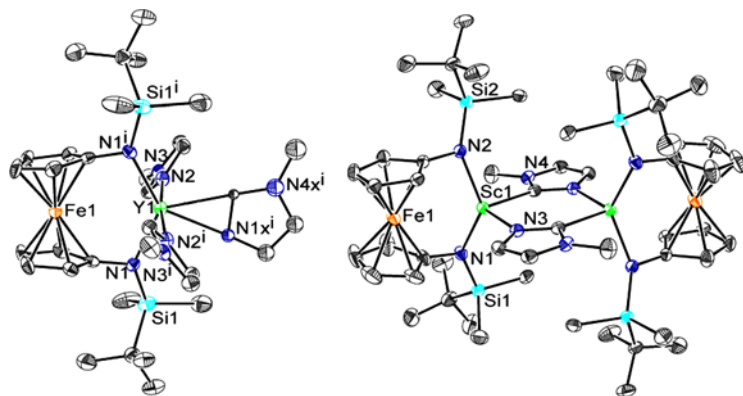


Figure 4. ORTEP representations (thermal ellipsoids at 50% probability) of  $2_{fc}^Y-(mi)_2$  (left) and  $[2_{fc}^{Sc}]_2$  (right); hydrogen atoms were removed for clarity. (Figure appears in color online.)

short iron–scandium distance of 3.08 Å, which is only 0.06 Å longer than the sum of the covalent radii of iron and scandium (3.02 Å).

In the case of 1-methylbenzimidazole, the scandium reaction was straightforward and led to the isolation of  $2_{fc}^{Sc}-mbi$ , which was also characterized by X-ray crystallography (Figure 5). In the analogous reactions

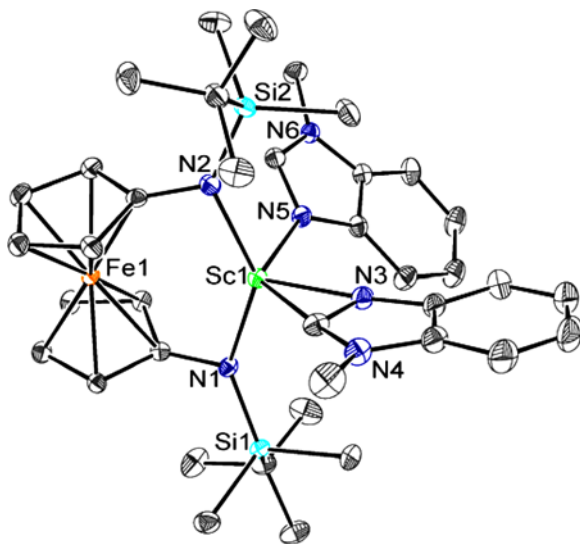
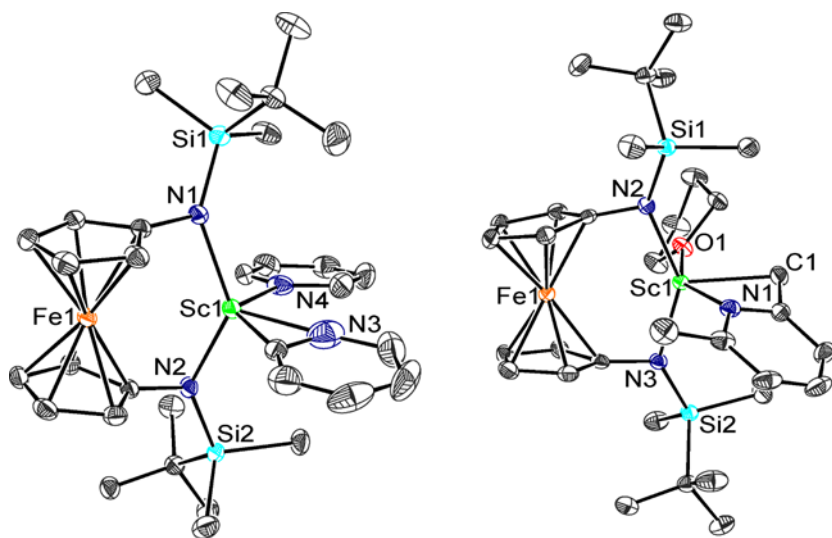
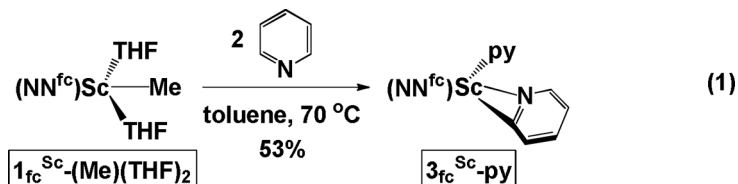


Figure 5. ORTEP representation (thermal ellipsoids at 50% probability) of  $2_{fc}^{Sc}-mbi$ ; hydrogen atoms were removed for clarity. (Figure appears in color online.)

with the yttrium and lutetium benzyl complexes, the formation of  $2^M_{fc}\text{-mbi}$  was observed by  $^1\text{H}$  NMR spectroscopy. Benzene or toluene solutions of  $2^M_{fc}\text{-mbi}$  ( $M = \text{Y, Lu}$ ) transformed, however, rapidly to the corresponding coupled products (see below) and the ortho-metalated complexes could not be isolated.

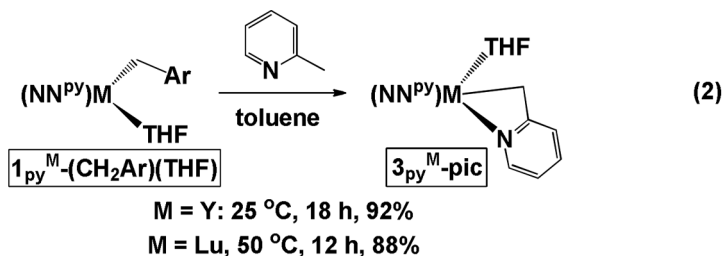
All benzyl complexes gave complicated reaction mixtures with pyridine,<sup>[53]</sup> but the scandium methyl complex  $1^{\text{Sc}}_{fc}\text{-(Me)(THF)}_2$  led to the expected C–H activated product,  $3^{\text{Sc}}_{fc}\text{-py}$  (Eq. 1).<sup>[65]</sup> The complex  $3^{\text{Sc}}_{fc}\text{-py}$  was characterized by X-ray crystallography, which indicated that the pyridyl and pyridine ligands were coplanar and coordinated in a plane perpendicular to the  $\text{N}_{\text{amide}}\text{FeN}_{\text{amide}}$  plane (Figure 6).



**Figure 6.** ORTEP representations (thermal ellipsoids at 50% probability) of  $3^{\text{Sc}}_{fc}\text{-py}$  (left) and  $3^{\text{Sc}}_{fc}\text{-lut}$  (right); hydrogen atoms were removed for clarity. (Figure appears in color online.)

When the pyridine was ortho-substituted, the C–H activation reaction proceeded smoothly with the benzyl complexes to give the expected ortho-metallated products  $3_{\text{fc}}^{\text{M}}$  (Scheme 2).<sup>[64]</sup> Interestingly, the C–H activation of 2-picoline by  $1_{\text{fc}}^{\text{M}}\text{-(CH}_2\text{Ph)(THF)}$  ( $\text{M} = \text{Y, La}$ ) gave exclusively  $3_{\text{fc}}^{\text{M}}\text{-pic}$ , featuring an  $\text{sp}^3\text{-C}_{\text{CH}_2}\text{-M}$  bond instead of an  $\text{sp}^2\text{-C}_{\text{pyridyl}}\text{-M}$  bond. Similar results have been reported for some yttrium<sup>[66]</sup> and thorium alkyl complexes.<sup>[67]</sup>

Although two isomers may exist for the THF adducts  $3_{\text{fc}}$  (with the exception of  $3_{\text{fc}}^{\text{Sc}}\text{-lut}$ ) depending on the relative orientation of the pyridyl and the coordinated THF ligand, only one isomer was observed in solution for all cases. Based on DFT calculations and  $^1\text{H}$  NMR spectroscopy experiments, it was found that either isomer was preferred for a specific heterocycle.<sup>[64]</sup> The Jordan group also reported that  $\eta^2\text{-N,C-pyridyl}$  zirconocene complexes existed as single isomers in solution, with the exception of quinoline and 7,8-benzoquinoline, when both isomers were observed.<sup>[68]</sup> The complex  $3_{\text{fc}}^{\text{Sc}}\text{-lut}$  was characterized by X-ray crystallography (Figure 6), which indicated a  $\kappa^3\text{-N,C,C-}$ coordination of lutidine.

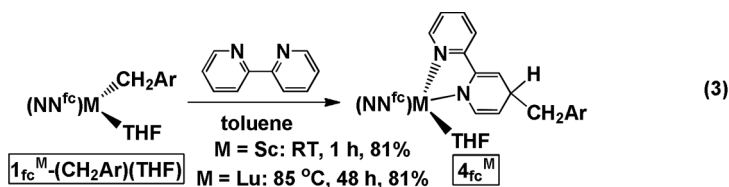


The reaction between the pincer complexes  $1_{\text{py}}^{\text{M}}\text{-(CH}_2\text{Ar)(THF)}$  and four equivalents of pyridine at  $50^\circ\text{C}$  gave a mixture of products, similar to what was observed when the corresponding ferrocene-diamide complexes were employed. Unlike the case for  $1_{\text{fc}}^{\text{M}}\text{-(CH}_2\text{Ar)(THF)}$  though, the reactions between  $1_{\text{py}}^{\text{M}}\text{-(CH}_2\text{Ar)(THF)}$  and 2-phenylpyridine or 8-methylquinoline also resulted in intractable mixtures of products.<sup>[55]</sup> A reaction sequence analogous to that observed for the ferrocene-diamide complexes was found only when 2-picoline was employed to give  $3_{\text{py}}^{\text{M}}\text{-pic}$  (Eq. 2).<sup>[55]</sup>

**3.2.2. Alkyl Transfer.** In an effort to extend the scope of the aromatic N-heterocycle ortho-metalation reaction<sup>[52,53,65]</sup> to biheterocyclic



substrates, the reactions of  $1_{fc}^M-(CH_2Ar)(THF)$  with 2,2'-bipyridine and isoquinoline were investigated. Instead of the C–H activation reaction encountered with pyridines and imidazoles, products of alkyl transfer to the heterocycle were observed.<sup>[54]</sup> Such a behavior was also reported for the reaction of  $Lu(CH_2SiMe_3)_3(THF)_2$  with 2,2':6',2''-terpyridine.<sup>[69]</sup>



In the case of 2,2'-bipyridine (Eq. 3), X-ray crystallography (Figure 7) indicated that the alkyl transfer occurred to the 4-position of a pyridine ring to give  $4_{fc}^M$  ( $M = Sc$ ).<sup>[54]</sup> It was proposed that an initial 1,3-alkyl transfer to the 6-position took place, similar to the 1,3-alkyl transfer from  $Lu(CH_2SiMe_3)_3(THF)_2$  to 2,2':6',2''-terpyridine,<sup>[69]</sup> and then an isomerization led to  $4_{fc}^M$ , likely the thermodynamically stable product.

The reaction of  $1_{fc}^M-(CH_2Ar)(THF)$  with isoquinoline revealed that a 1,3-alkyl migration of the benzyl group onto the  $\alpha$ -carbon of isoquinoline

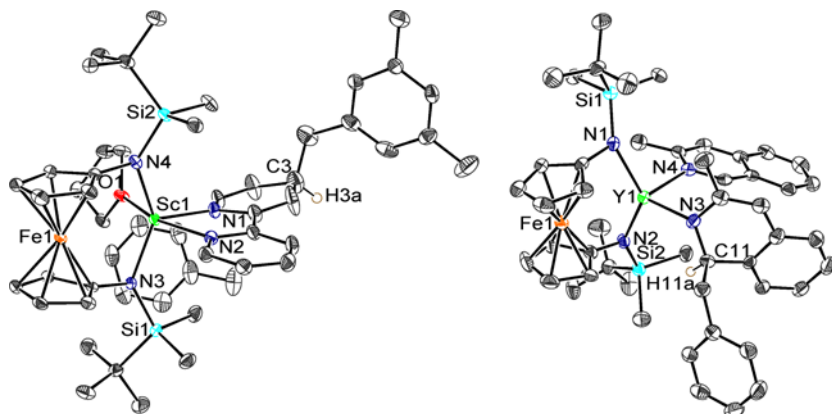
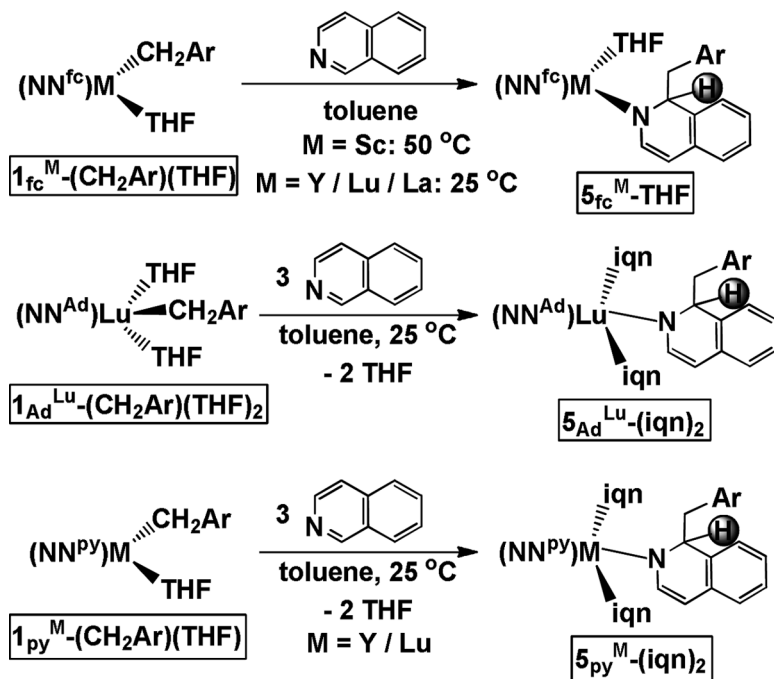


Figure 7. ORTEP representations (thermal ellipsoids at 50% probability) of  $4_{fc}^{Sc}$  (left) and  $5_{fc}^{Y-iqu}^{Me}$  (right); irrelevant hydrogen atoms were removed for clarity. (Figure appears in color online.)



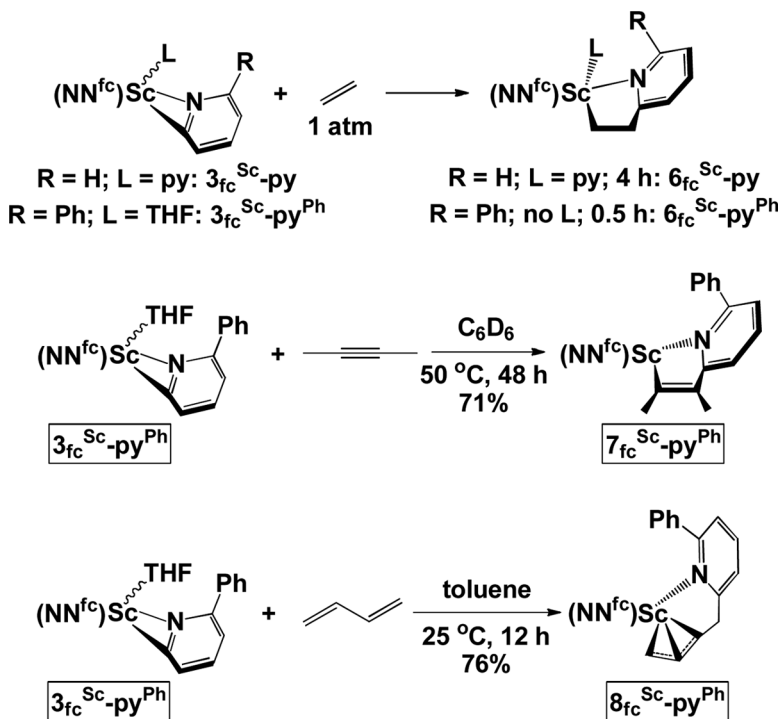
Scheme 3. Reactions of isoquinoline with  $1_{\text{NN}}^{\text{M}}\text{-(CH}_2\text{Ar)(THF)}$ .

took place at room temperature ( $\text{M} = \text{Y, Lu, La}$ ) or  $50^\circ\text{C}$  ( $\text{M} = \text{Sc}$ ), resulting in the formation of  $5_{\text{fc}}^{\text{M}}\text{-THF}$  (Scheme 3). The yttrium complex,  $5_{\text{fc}}^{\text{Y}}\text{-iqn}^{\text{Me}}$ , in which isoquinoline and THF were replaced by 3-methylisoquinoline ( $\text{iqn}^{\text{Me}}$ ), was characterized by X-ray crystallography (Figure 6), which confirmed that the alkyl transfer occurred to the 1-position of isoquinoline. The complexes  $1_{\text{Ad}}^{\text{Lu}}\text{-(CH}_2\text{Ar)(THF)}_2$  and  $1_{\text{py}}^{\text{M}}\text{-(CH}_2\text{Ar)(THF)}$  also reacted with three equivalents of isoquinoline in toluene at room temperature to give  $5_{\text{Ad}}^{\text{Lu}}\text{-(iqn)}_2$  and  $5_{\text{py}}^{\text{M}}\text{-(iqn)}_2$ , respectively (Scheme 3). DFT calculations on a ferrocene-diamide yttrium model system showed that a late transition state was operating for the alkyl-transfer reaction, with the benzyl carbon migrating as a carbanion and almost completely detached from the metal, while the receiving pyridine was partially dearomatized at the potential energy saddle point.<sup>[54]</sup>

**3.2.3. Insertion Reactions.** Methods to functionalize heterocycles have been of longstanding interest given the ubiquitous presence of these

structures in biological compounds.<sup>[70–77]</sup> Pioneered by Jordan in the early 1990s,<sup>[59,78–80]</sup> the functionalization of N-heterocycles using early transition metal alkyl complexes has found numerous applications.<sup>[81–93]</sup> These reactions usually involve the migratory insertion of an unsaturated substrate into the metal-carbon bond of a strained metallaziridine and the formation of a new four- or five-member ring metallocycle.

The reaction between  $3_{\text{fc}}^{\text{Sc}}\text{-py}$  and ethylene occurred at room temperature in 4 hours and led to the insertion product  $6_{\text{fc}}^{\text{Sc}}\text{-py}$  (Scheme 4). It was not surprising that the reaction was rather slow since the analogous zirconocene pyridyl cationic complex featuring a pyridine molecule coordinated to the metal center did not react with ethylene.<sup>[78]</sup> Given the low reactivity of  $3_{\text{fc}}^{\text{Sc}}\text{-py}$ , we decided to focus on a different complex. Jordan et al. showed that using the steric pressure of a methyl substituent close to the metal center increased the rate of the insertion

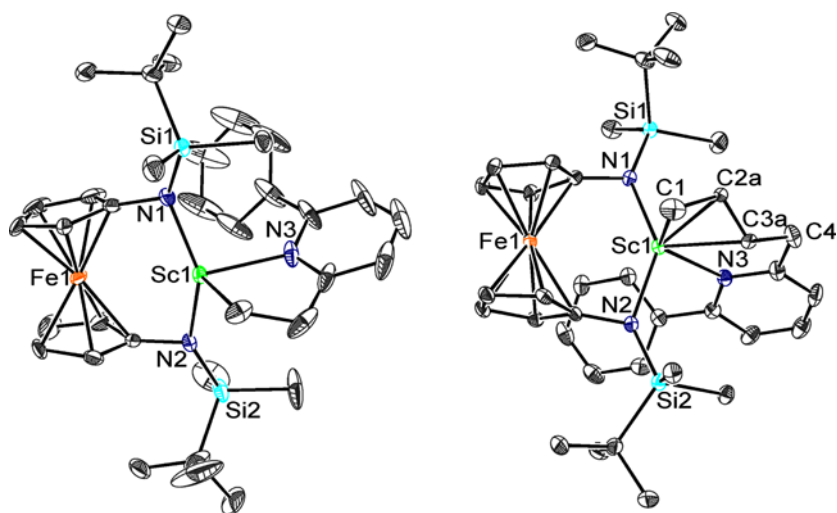


Scheme 4. Migratory-insertion reactions of unsaturated substrates with scandium pyridyl complexes.

reactions.<sup>[78,94,95]</sup> Indeed, when the phenylpyridyl complex  $3_{\text{fc}}^{\text{Sc}}\text{-py}^{\text{Ph}}$  was used instead of  $3_{\text{fc}}^{\text{Sc}}\text{-py}$ , the same reaction took place in half an hour (Scheme 4) to give  $6_{\text{fc}}^{\text{Sc}}\text{-py}^{\text{Ph}}$  (Figure 8).

The reactions of  $6_{\text{fc}}^{\text{Sc}}\text{-py}^{\text{Ph}}$  with 2-butyne to give  $7_{\text{fc}}^{\text{Sc}}\text{-py}^{\text{Ph}}$  and 1,3-butadiene to give  $8_{\text{fc}}^{\text{Sc}}\text{-py}^{\text{Ph}}$  were carried out (Scheme 4) in order to compare the reactivity of scandium pyridyl complexes with the reactivity of analogous yttrocene and zirconocene complexes. The formation of  $7_{\text{fc}}^{\text{Sc}}\text{-py}^{\text{Ph}}$  is analogous to the reaction of the zirconocene pyridyl cationic complex reported by Jordan et al. and 2-butyne.<sup>[78]</sup> The yttrocene pyridyl complex reported by Teuben et al. showed, however, a different reactivity behavior: instead of an insertion reaction, a deprotonation reaction involving the methyl butyne protons took place.<sup>[96]</sup>

With respect to the reaction between  $6_{\text{fc}}^{\text{Sc}}\text{-py}^{\text{Ph}}$  and 1,3-butadiene, Teuben reported that butadiene did not react with the yttrium complex  $\text{Cp}^*_2\text{Y}(\eta^2\text{-}N,C\text{-pyridyl})$ .<sup>[96]</sup> No information related to a reaction of butadiene with the zirconium cationic pyridyl complexes could be found in the reports published by Jordan.<sup>[78]</sup> The product  $8_{\text{fc}}^{\text{Sc}}\text{-py}^{\text{Ph}}$  was crystallographically characterized (Figure 8). The carbon atoms of the allyl backbone were disordered, showing two different orientations for the



**Figure 8.** ORTEP representations of  $6_{\text{fc}}^{\text{Sc}}\text{-py}^{\text{Ph}}$  (left, thermal ellipsoids at 35% probability) and  $8_{\text{fc}}^{\text{Sc}}\text{-py}^{\text{Ph}}$  (right, only one of the allyl orientations shown; thermal ellipsoids at 50% probability); hydrogen atoms were removed for clarity. (Figure appears in color online.)

allyl ligand, analogously to the disorder reported by Bercaw et al. for a non-substituted allyl scandocene complex.<sup>[97]</sup>

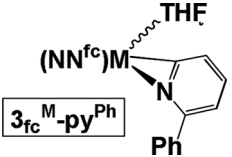
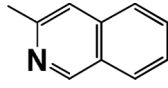
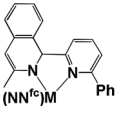

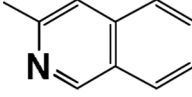
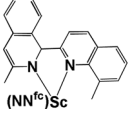
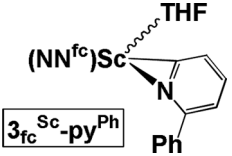
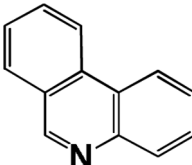
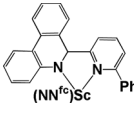
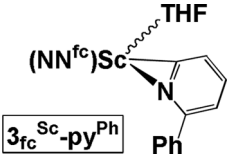
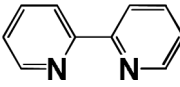
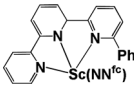
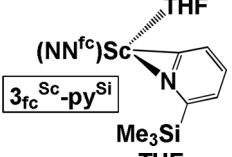
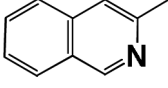
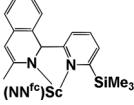
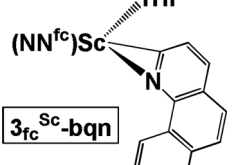
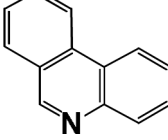
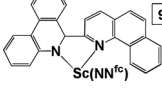
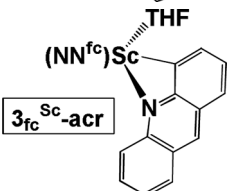
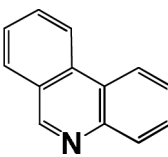
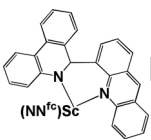
**3.2.4. Coupling.** Although the migratory insertions of unsaturated substrates with the scandium pyridyl complexes described above were expected, the formation of C–C coupling products from the reactions of the newly synthesized pyridyl complexes  $3_{fc}^M$  with pyridines, described below, was unexpected. As mentioned, the reaction between  $1_{fc}^M$ -(CH<sub>2</sub>Ar)(THF) and excess pyridine gave a mixture of products; it was identified that the mixture showed signals in the olefinic region of its <sup>1</sup>H NMR spectrum. When ortho-substituted pyridines were employed, however, the C–C coupling reaction proved remarkably general ( $9_{fc}^M$ , Table 5). The coupling reaction was not observed before, but it was proposed as a step in the formation of 2,2'-bipyridine from Cp<sub>2</sub>Y( $\eta^2$ -N,C-pyridyl) and excess pyridine.<sup>[96]</sup> The ferrocene-diamide ligands proved extremely versatile in supporting a variety of such products, while the pyridine diamide used was featured in only one case. The explanation for this behavior may be dependent on the pincer diamide's inability to lead to clean ortho-metalated complexes and on the ancillary ligand's ability to support the products of the C–C coupling reaction.<sup>[55]</sup>

The complexes  $9_{fc}^{Sc}$ -py<sup>Ph</sup>-py<sup>Ph</sup>,  $9_{fc}^{Sc}$ -py<sup>Ph</sup>-iqn,  $9_{fc}$ -py<sup>Ph</sup>-phan, and  $9_{fc}$ -acr-phan were crystallographically characterized (Figure 9). All solid-state structures were consistent with the dearomatization of one of the heterocycles by showing distances to the sp<sup>3</sup>-hybridized carbon atom lengthened in the coupled complexes versus distances expected for an aromatic ring, and angles indicative of a pseudo-tetrahedral geometry at that carbon atom. The two heteroaromatic rings are almost coplanar in the first three complexes ( $9_{fc}^{Sc}$ -py<sup>Ph</sup>-py<sup>Ph</sup>,  $9_{fc}^{Sc}$ -py<sup>Ph</sup>-iqn, and  $9_{fc}$ -py<sup>Ph</sup>-phan). Because of the larger size of the ring formed by coupling in  $9_{fc}$ -acr-phan than in the other three complexes (six versus five atoms), the two bulky heterocycles in  $9_{fc}$ -acr-phan could adopt a perpendicular orientation relative to each other. The increased flexibility of the six-member ring in  $9_{fc}$ -acr-phan also allowed the biheterocyclic fragment to come in close proximity to the metal center.

Several factors were found to promote the coupling reactions of the C–H activated complexes  $3_{fc}^M$  with pyridine substrates:<sup>[64]</sup>

1. Ortho-substituents accelerated the coupling reaction, although large substituents inhibited it.

Table 5. Coupling of aromatic N-heterocycles<sup>a</sup>

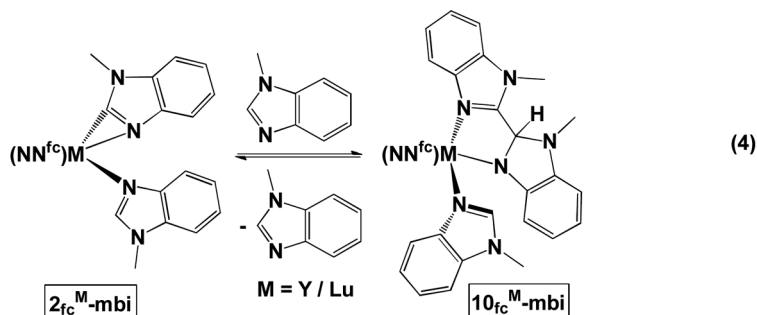
Compound	Substrate	Product
 $3_{fc}^M\text{-py}^{\text{Ph}}$		 $9_{fc}^M\text{-py}^{\text{Ph}}\text{-ign}^{\text{Me}}$ $M = \text{Sc} / \text{Y} / \text{Lu}$
 $3_{fc}^{\text{Sc}}\text{-qn}^{\text{Me}}$		 $9_{fc}^{\text{Sc}}\text{-qn}^{\text{Me}}\text{-ign}^{\text{Me}}$
 $3_{fc}^{\text{Sc}}\text{-py}^{\text{Ph}}$		 $9_{fc}^{\text{Sc}}\text{-py}^{\text{Ph}}\text{-phan}$
 $3_{fc}^{\text{Sc}}\text{-py}^{\text{Ph}}$		 $9_{fc}^{\text{Sc}}\text{-py}^{\text{Ph}}\text{-bipy}$
 $3_{fc}^{\text{Sc}}\text{-py}^{\text{Si}}$		 $9_{fc}^{\text{Sc}}\text{-py}^{\text{Si}}\text{-ign}^{\text{Me}}$
 $3_{fc}^{\text{Sc}}\text{-bqn}$		 $9_{fc}^{\text{Sc}}\text{-bqn-phan}$
 $3_{fc}^{\text{Sc}}\text{-acr}$		 $9_{fc}^{\text{Sc}}\text{-acr-phan}$

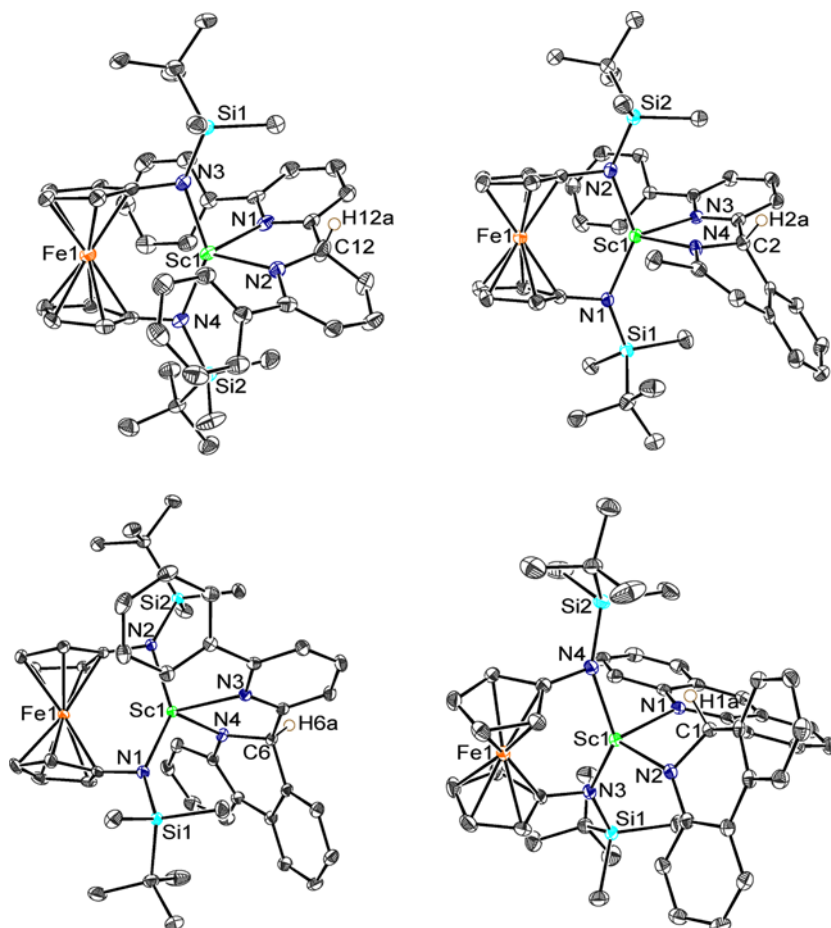
<sup>a</sup>All reactions occurred in toluene or toluene/*n*-pentane at room temperature.

2. The use of chelating substrates was beneficial.
3. Fused aromatic rings on the coupling partner had an accelerating effect.

It became apparent that the coupling reaction was not restricted to  $\eta^2$ -N,C-pyridyl complexes when an analogous reaction was observed from the  $\text{CH}_2$  group of  $3^{\text{Sc}}_{\text{fc}}\text{-lut}$  (Scheme 5). The reaction of  $3^{\text{Sc}}_{\text{fc}}\text{-lut}$  with 3-methylisoquinoline led to a coupled product,  $9^{\text{Sc}}_{\text{fc}}\text{-lut-iqn}^{\text{Me}}$ , in which the two heterocyclic rings were bridged by a methylene group. The formation of  $9^{\text{Sc}}_{\text{fc}}\text{-lut-iqn}^{\text{Me}}$  was not an isolated example and the yttrium and lanthanum compounds obtained by the C–H activation of 2-picoline,  $3^{\text{M}}_{\text{NN}}\text{-pic}$  ( $\text{NN} = \text{NN}^{\text{fc}}$ ,  $\text{M} = \text{Y, La}$ ;  $\text{NN} = \text{NN}^{\text{py}}$ ,  $\text{M} = \text{Y}$ ), also reacted with 3-methylisoquinoline to give  $9^{\text{M}}_{\text{NN}}\text{-pic-iqn}^{\text{Me}}$ . Furthermore,  $3^{\text{Sc}}_{\text{fc}}\text{-py}^{\text{Et}}$ , a compound which contains a  $\text{Sc-CH}_2\text{CH}_2\text{-pyridine}$  motif,<sup>[65]</sup> also reacted with 3-methylisoquinoline to give the coupling product  $9^{\text{Sc}}_{\text{fc}}\text{-py}^{\text{Et}}\text{-iqn}^{\text{Me}}$ , in which the two heterocycles were bridged by a 1,2-ethylene group.<sup>[64]</sup>

The ortho-metalated imidazolyl complexes also showed C–C coupling reactivity. For 1-methylimidazole, the product of coupling with a coordinated imidazole ligand in  $2^{\text{Sc}}_{\text{fc}}\text{-(mi)}_2$  was proposed to be an intermediate in the ring opening reaction discussed below. Although the reaction of 1-methylbenzimidazole with  $1^{\text{Sc}}_{\text{fc}}\text{-(CH}_2\text{Ar)}(\text{THF})$  led only to the isolation of the  $\eta^2$ -N,C-imidazolyl complex  $2^{\text{Sc}}_{\text{fc}}\text{-mbi}$ , the reaction with the larger analogues,  $1^{\text{M}}_{\text{fc}}\text{-(CH}_2\text{Ar)}(\text{THF})$  ( $\text{M} = \text{Y, Lu}$ ), allowed the observation of the C–C coupled product  $10^{\text{M}}_{\text{fc}}\text{-mbi}$  (Eq. 4), which was crystallographically characterized (Figure 10). Interestingly, the formation of the C–C bond in  $10^{\text{M}}_{\text{fc}}\text{-mbi}$  was reversible,<sup>[98]</sup> as shown by variable-temperature  $^1\text{H}$  NMR spectroscopy and DFT calculations.<sup>[99]</sup>

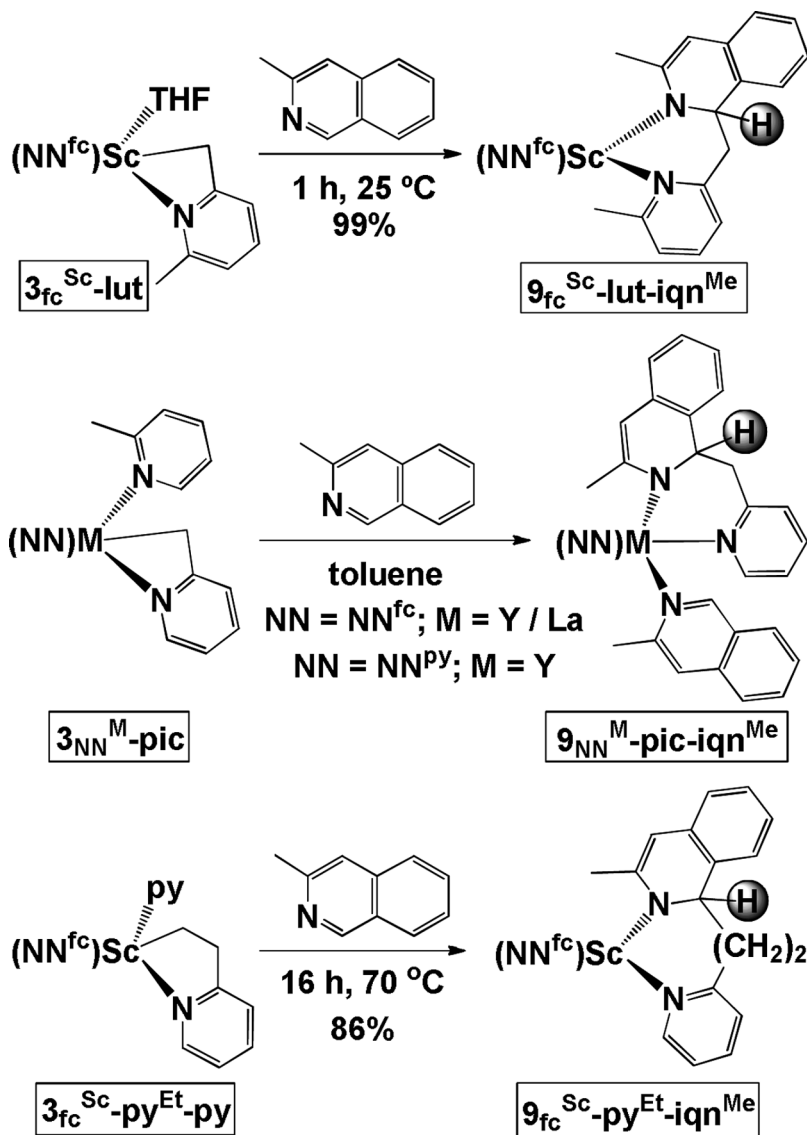




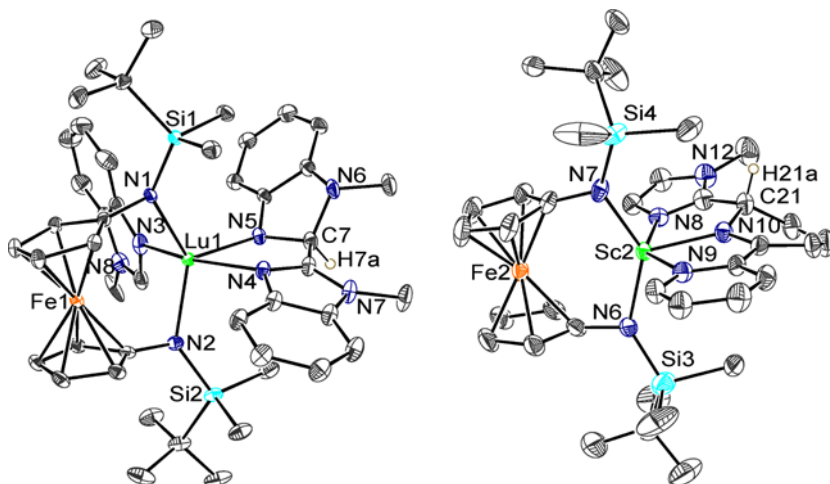
**Figure 9.** ORTEP representations (thermal ellipsoids at 50% probability) of  $9^{\text{Sc}}_{\text{fc}}\text{-py}^{\text{Ph}}\text{-py}^{\text{Ph}}$ ,  $9^{\text{Sc}}_{\text{fc}}\text{-py}^{\text{Ph}}\text{-iqu}$ ,  $9^{\text{Sc}}_{\text{fc}}\text{-py}^{\text{Ph}}\text{-phan}$ , and  $9^{\text{Sc}}_{\text{fc}}\text{-acr-phan}$ ; irrelevant hydrogen atoms were removed for clarity. (Figure appears in color online.)

Efforts were made to isolate coupling products from the C–H-activated 1-methylimidazole ligands. Neither  $2^{\text{Sc}}_{\text{fc}}\text{-mi}$  nor  $[2^{\text{Sc}}_{\text{fc}}]_2$  reacted with pyridines; however, both complexes reacted with 2,2'-bipyridine at 50°C and yielded a bright red-orange coupled product,  $10^{\text{Sc}}_{\text{fc}}\text{-mi-bipy}$  (Eq. 5). The complex  $10^{\text{Sc}}_{\text{fc}}\text{-mi-bipy}$  was characterized by X-ray crystallography (Figure 10).

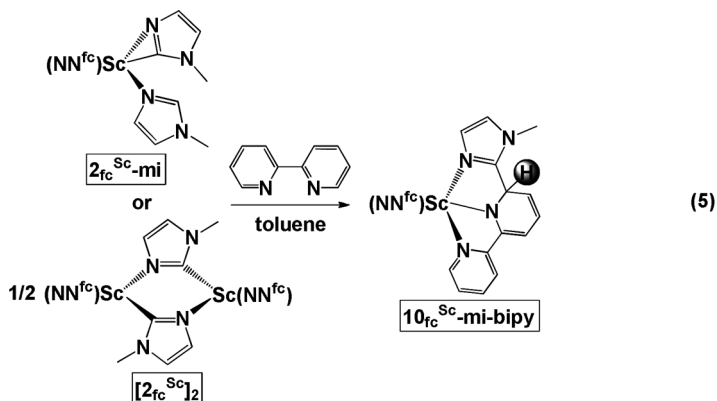




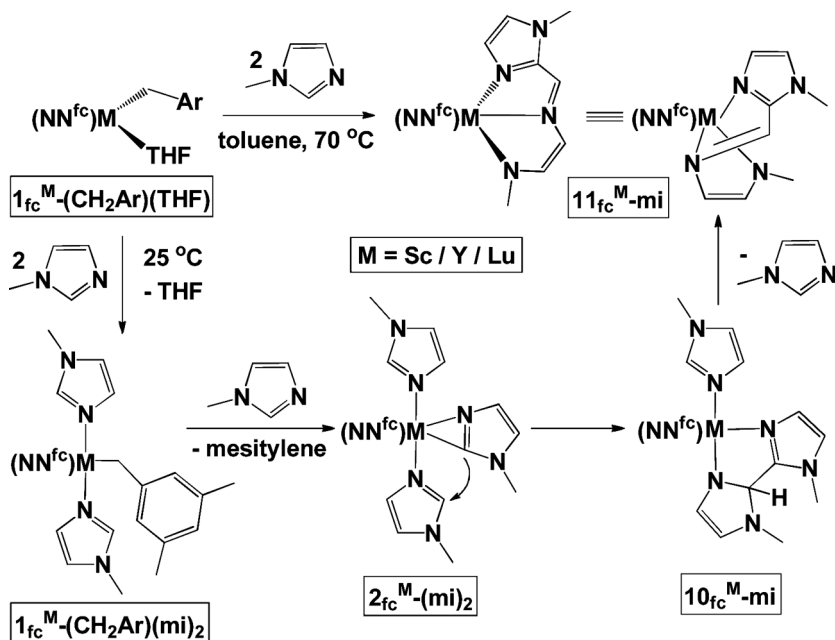
Scheme 5. Coupling of methylene- and ethylene-pyridine complexes with 3-methyloquinoline.



**Figure 10.** ORTEP representations of  $10^{\text{Lu}}\text{-mbi}$  (thermal ellipsoids at 50% probability) and  $10^{\text{Sc}}\text{-mi-bipy}$  (thermal ellipsoids at 35% probability); irrelevant hydrogen atoms were removed for clarity. (Figure appears in color online.)



**3.2.5. Ring Opening.** The reaction mixture obtained from  $1^{\text{Sc}}\text{-(CH}_2\text{Ar)}(\text{THF})$  and three equivalents of 1-methylimidazole (Scheme 6) turned, surprisingly, from a yellow/light-orange to a dark-purple color after heating it for several hours at  $70^\circ\text{C}$ . The isolated product was characterized as  $11^{\text{Sc}}\text{-mi}$  by X-ray crystallography (Figure 10) and contained an imidazole-imine-amide moiety, in which one imidazole fragment was ring opened. Other examples of homogeneous systems that

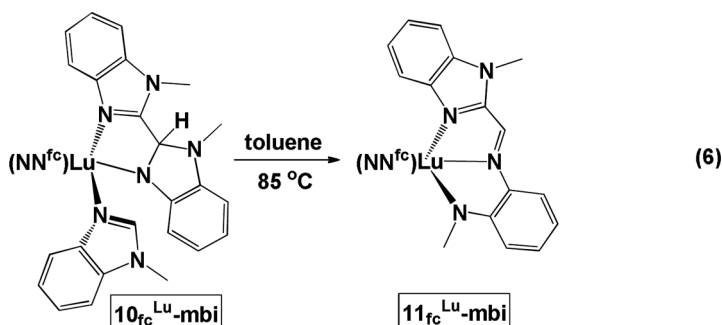


Scheme 6. Ring opening of 1-methylimidazole by  $1_{fc}^M-(CH_2Ar)(THF)$  ( $M = Sc, Y, Lu$ ).

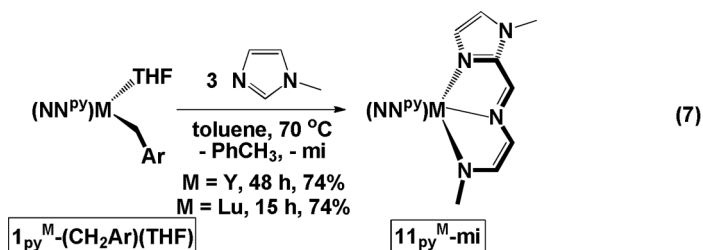
mediate the ring opening of aromatic N-heterocycles are also based on early transition metals such as tantalum,<sup>[100]</sup> niobium,<sup>[101,102]</sup> and titanium,<sup>[103,104]</sup> with the exception of a rhenium system,<sup>[105,106]</sup> which employs external bases and electrophilic reagents, and a low-valent tungsten complex that breaks the C–C bond of quinoxaline.<sup>[107]</sup> Actinide complexes have also been shown to effect the ring opening of aromatic N-heterocycles,<sup>[108–110]</sup> as reported by the Kiplinger group for thorium and pyridine-N-oxides<sup>[111]</sup> and by the Gambarotta group, when redox processes contribute to pyrazole ring opening by uranium centers.<sup>[112]</sup>

The ring opening of 1-methylimidazole was found to be mediated by all ferrocene-diamide complexes ( $1_{fc}^M-(CH_2Ar)(THF)$  and  $1_{Ad}^{Lu}-(CH_2Ar)(THF)_2$ ).<sup>[52,53,57]</sup> The following mechanism was proposed based on NMR spectroscopy and X-ray crystallography studies (Scheme 6).<sup>[53]</sup> The first step involves displacement of THF and coordination of two imidazole molecules. The C–H activation of one of the 1-methylimidazole ligands to give  $2_{fc}^M-(mi)_2$  is the slow step of the entire process. Following C–H activation, C–C coupling<sup>[96]</sup> between the  $\eta^2$ -N,C-imidazolyl and

one of the coordinated imidazoles occurs and is accompanied by the dearomatization of one of the rings to give  $10_{fc}^M\text{-mi}$ , as mentioned above. That intermediate was not observed and it was proposed that it transformed into the final product  $11_{fc}^M\text{-mi}$ , likely stabilized by extended conjugation. The above mechanistic scheme was supported by DFT calculations.<sup>[53]</sup> In addition to providing information about the ring-opening step, the calculations revealed that the dearomatized 1-methylimidazole fragment must undergo a rotation to allow the coordination of the nitrogen bearing the methyl group. This rotation showed the highest activation barrier of the calculated process.<sup>[53]</sup>

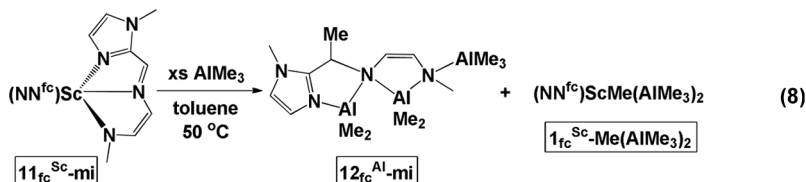


The reactions between  $1_{fc}^M\text{-(CH}_2\text{Ar)}(\text{THF})$  and 1-methylbenzimidazole (mbi) provided further support for the proposed mechanism.<sup>[99]</sup> As described above, the C–C coupled product  $10_{fc}^{\text{Lu}}\text{-mbi}$  was isolated and crystallographically characterized (Eq. 4 and Figure 10). The complex  $10_{fc}^{\text{Lu}}\text{-mbi}$  transformed into the expected ring-opened product,  $11_{fc}^{\text{Lu}}\text{-mbi}$  (Eq. 6), by prolonged heating at 85 °C.<sup>[99]</sup>



The ring opening of 1-methylimidazole was found to be mediated also by the pyridine-diamide complexes  $1_{py}^M\text{-(CH}_2\text{Ar)}(\text{THF})$ . The reaction between  $1_{py}^Y\text{-(CH}_2\text{Ph)}(\text{THF})$  or  $1_{py}^{\text{Lu}}\text{-(CH}_2\text{Ar)}(\text{THF})$  and three equivalents of 1-methylimidazole (Eq. 7) resulted in the formation of

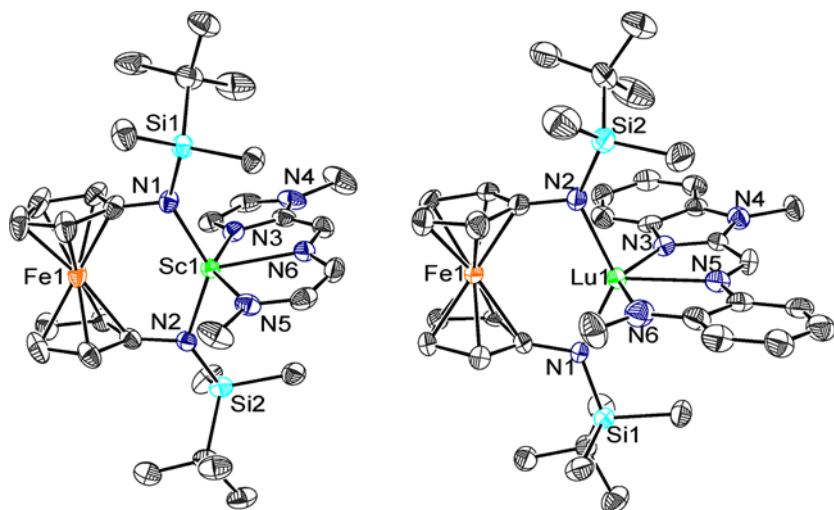
$11^M_{\text{py-mi}}$ , analogously to what was observed for the ferrocene-based complexes.<sup>[55]</sup> We proposed that a similar mechanism operated in those transformations as well. The reactions with 1-methylbenzimidazole, however, did not proceed cleanly for the pyridine-diamide complexes.



Given the unusual planar, tridentate nature of the imidazole-imine-amide ligand in  $11^M_{\text{fc-mi}}$ , we became interested in determining whether this fragment can be removed from M and used as a ligand for a different metal. In addition to transferring the imidazole-imine-amide unit of  $11^M_{\text{fc-mi}}$  to another metal, transmetalation would allow the recycling of the metal ferrocene-diamide fragment. The reaction of the scandium complex  $11^{\text{Sc}}_{\text{fc-mi}}$  with 8 equivalents of  $\text{AlMe}_3$  led to the formation of two major products (Eq. 8).<sup>[113]</sup> The products were separated and isolated based on their different solubility properties: a hexanes extraction led to the previously reported  $(\text{NN}^{\text{fc}})\text{ScMe}(\text{AlMe}_3)_2$  ( $1^{\text{Sc}}_{\text{fc-Me}}(\text{AlMe}_3)_2$ ),<sup>[51]</sup> while a toluene extraction allowed the isolation of a colorless solid, which was identified by NMR spectroscopy, X-ray crystallography (Figure 12), and elemental analysis as the trialuminum complex  $12^{\text{Al}}_{\text{fc-mi}}$ .<sup>[113]</sup>

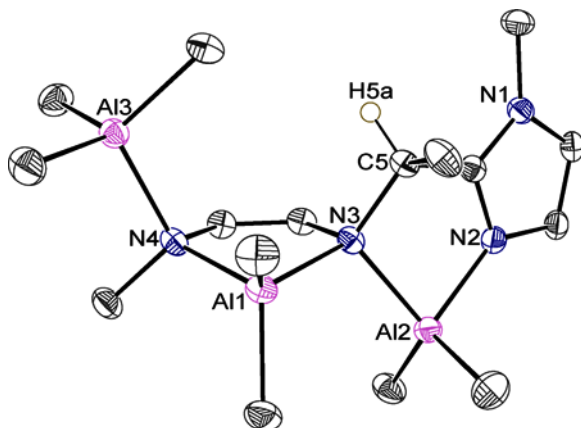
### 3.2.6. Hydrogen-Transfer Processes

**3.2.6.1. Isomerization of  $9^M_{\text{fc}}$ :** Since the mechanism of imidazole ring opening involves a coupled product as an intermediate, the reactivity of the pyridine-coupled products was also tested. Solutions of  $9^M_{\text{fc-py}}^{\text{Ph-iqu}}$  ( $M = \text{Sc}, \text{Y}, \text{Lu}$ ) were heated at 70 or 85 °C for several days, during which time their color changed from red to green (Scheme 7). All  $9^M_{\text{fc-py}}^{\text{Ph-iqu}}$  compounds transformed with at least 60% conversion into  $13^M_{\text{fc-py}}^{\text{Ph-iqu}}$  (Figure 13,  $M = \text{Sc}$ ), in which a different carbon of the dearomatized ring became  $\text{sp}^3$ .<sup>[53]</sup> The isomerization by 1,4-hydrogen transfer was also observed for the coupled product of 2-phenylpyridine with 2-picoline ( $9^{\text{Sc}}_{\text{fc-py}}^{\text{Ph-pic}}$ ) or of 8-methylquinoline with 3-methylisoquinoline ( $9^{\text{Sc}}_{\text{fc-qn}}^{\text{Me-iqu}^{\text{Me}}}$ ) that transformed to  $13^{\text{Sc}}_{\text{fc-py}}^{\text{Ph-pic}}$  and  $13^{\text{Sc}}_{\text{fc-qn}}^{\text{Me-iqu}^{\text{Me}}}$ , respectively, upon heating. In the case of  $13^{\text{Sc}}_{\text{fc-py}}^{\text{Ph-pic}}$ , the coupling product  $9^{\text{Sc}}_{\text{fc-py}}^{\text{Ph-pic}}$  could not be isolated because its formation was competitive with its isomerization. Those additional reactions were

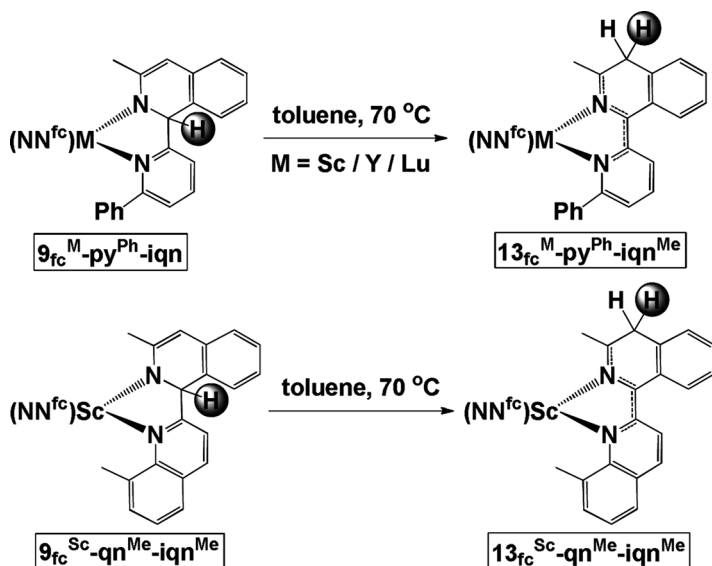


**Figure 11.** ORTEP representations of  $11^{\text{Sc}}_{\text{mi}}$  (thermal ellipsoids at 35% probability) and  $11^{\text{Lu}}_{\text{mbi}}$  (thermal ellipsoids at 50% probability); hydrogen atoms were removed for clarity. (Figure appears in color online.)

limited to scandium complexes because mixtures of products that proved intractable were obtained for yttrium and lutetium. Other biheterocyclic complexes  $9^{\text{M}}_{\text{fc}}$  could be obtained, but the heating of their solutions also gave unsolvable mixtures of products. In some of those mixtures,



**Figure 12.** ORTEP representation (thermal ellipsoids at 50% probability) of  $12^{\text{Al}}_{\text{mi}}$ ; irrelevant hydrogen atoms were removed for clarity. (Figure appears in color online.)



Scheme 7. Isomerization of biheterocyclic ligands in  $9_{\text{fc}}^{\text{M}}$ .

complexes of the type  $13_{\text{fc}}^{\text{M}}$  could be identified by  $^1\text{H}$  NMR spectroscopy, but their separation and isolation were not successful.

Mechanistic information was obtained from a cross-over experiment between  $9_{\text{fc}}^{\text{Sc}}-\text{qn}^{\text{Me}}-\text{iqu}^{\text{Me}}-d_4$  and  $9_{\text{fc}}^{\text{Sc}}-\text{py}^{\text{Ph}}-\text{iqu}^{\text{Me}}$  (Eq. 9). The experiment showed that there was no deuterium incorporation in  $13_{\text{fc}}^{\text{Sc}}-\text{py}^{\text{Ph}}-\text{iqu}^{\text{Me}}$ ,

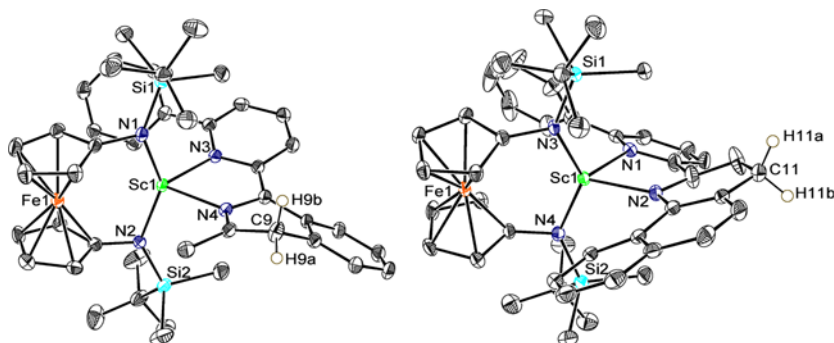
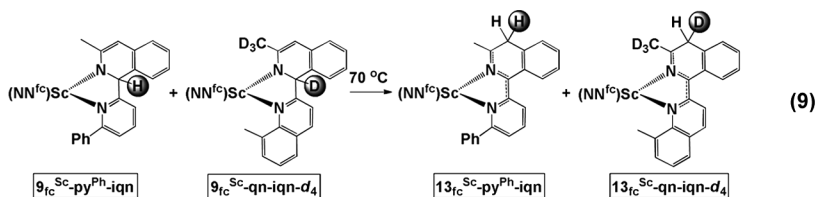


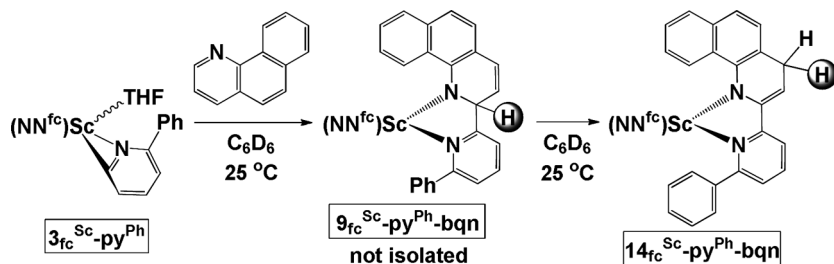
Figure 13. ORTEP representations (thermal ellipsoids at 50% probability) of  $13_{\text{fc}}^{\text{Sc}}-\text{py}^{\text{Ph}}-\text{iqu}$  (left) and  $14_{\text{fc}}^{\text{Sc}}-\text{py}^{\text{Ph}}-\text{bqn}$  (right); irrelevant hydrogen atoms were removed for clarity. (Figure appears in color online.)

indicating that the isomerization reaction was an intramolecular process. The intramolecular nature of the transformation was also supported by two other observations: (1) reactions in the presence of excess 3-methyloisoquinoline did not proceed at a different rate than reactions run in its absence; and (2) the addition of  $\text{Et}_3\text{N}$  to  $9_{\text{fc}}^{\text{Sc}}\text{-qn}^{\text{Me}}\text{-iqn}^{\text{Me}}$  did not influence the rate of the isomerization process.



The mechanism for the isomerization of  $9_{\text{fc}}^{\text{Sc}}\text{-py}^{\text{Ph}}\text{-iqn}$  to  $13_{\text{fc}}^{\text{Sc}}\text{-py}^{\text{Ph}}\text{-iqn}$  was also explored using DFT calculations. It was found that a direct transfer from C2 to C4 was the most energetically favored pathway. The proposed avenue involved a transition structure in which the hetero cycle adopted a boat-like conformation that facilitated the direct proton transfer.<sup>[53]</sup>

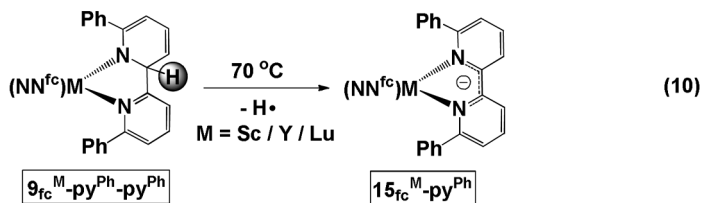
During the study of the coupling reaction between  $3_{\text{fc}}^{\text{Sc}}\text{-py}^{\text{Ph}}$  and 7,8-benzoquinoline, it was found that the coupled product  $9_{\text{fc}}^{\text{Sc}}\text{-py}^{\text{Ph}}\text{-bqn}$  formed very slowly (Scheme 8). Before the formation of  $9_{\text{fc}}^{\text{Sc}}\text{-py}^{\text{Ph}}\text{-bqn}$  was complete, however, the formation of a second,  $C_s$ -symmetric product was observed. The final product was identified as  $14_{\text{fc}}^{\text{Sc}}\text{-py}^{\text{Ph}}\text{-bqn}$  (Figure 13), in which the  $\text{sp}^3$ -hydrogen atom migrated to the benzyl carbon of the dearomatized pyridine ring (Scheme 8).<sup>[64]</sup> This isomerization reaction is a 1,3- as opposed to a 1,4-hydrogen migration, and it can be explained by the fact that the aromaticity of the naphthalene moiety is preserved in  $14_{\text{fc}}^{\text{Sc}}\text{-py}^{\text{Ph}}\text{-bqn}$ .



Scheme 8. Isomerization of the biheterocyclic ligand in  $9_{\text{fc}}^{\text{Sc}}\text{-py}^{\text{Ph}}\text{-bqn}$ .



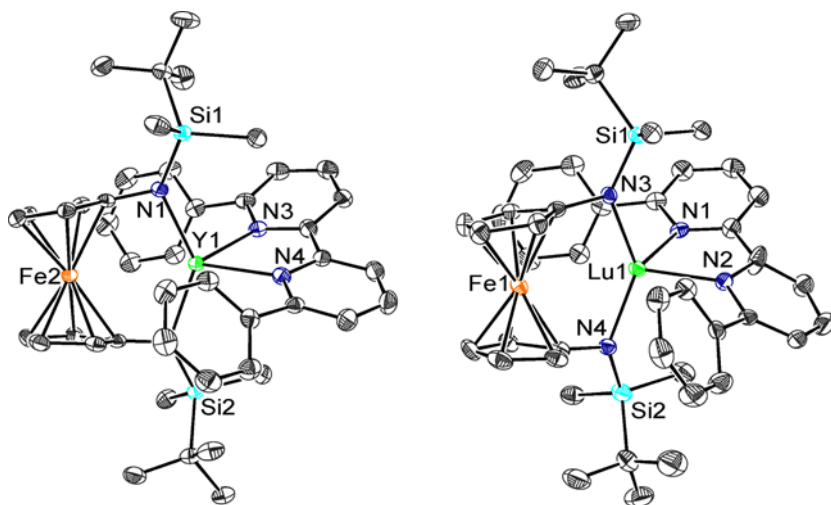
3.2.6.2. Hydrogen-transfer processes from  $9_{fc}^M$ : It was found that a certain class of coupled products,  $9_{fc}^M\text{-py}^{\text{Ph}}\text{-py}^{\text{Ph}}$  ( $M = \text{Sc}, \text{Y}, \text{Lu}$ ), undergoes a different type of hydrogen transfer (Eq. 10): heating those complexes caused the formation of complexes containing a radical-anionic 2,2'-bipyridyl ligand ( $15_{fc}^M\text{-py}^{\text{Ph}}$ ).<sup>[114]</sup> This method constitutes a new way of generating such complexes since it does not involve electron transfer to neutral 2,2'-bipyridyl or salt metathesis between the lithium salt of the 2,2'-bipyridyl radical anion and group 3 metal halides. It was also shown that, as expected, the use of an H- acceptor, 2,4,6-tri-*t*-butylphenoxy, led to high conversions (76% after recrystallization for yttrium versus 47% in the absence of the radical) and almost no byproduct formation.<sup>[114]</sup>



The X-ray crystal structures of  $15_{fc}^{\text{Y}}\text{-py}^{\text{Ph}}$  and  $15_{fc}^{\text{Lu}}\text{-py}^{\text{Ph}}$  were determined (Figure 14) and confirmed the radical anionic character of the bipyridyl ligand. All new bipy metal complexes were characterized by EPR and absorption spectroscopy. DFT calculations were used to probe the electronic structure of these compounds. All these methods support the radical-anionic character of bipy in all compounds.

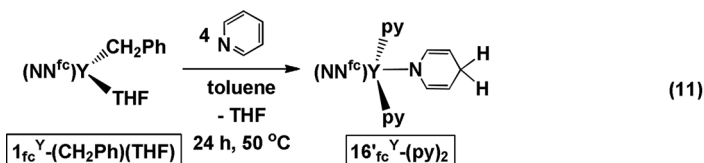
3.2.6.3. Hydrogen-transfer processes from  $5_{NN}^M$ : During the course of the reaction of  $1_{fc}^M\text{-(CH}_2\text{Ar)(THF)}$  with isoquinoline, it was observed that employing an excess of substrate led to the formation of a new product,  $16_{fc}^M\text{-(iqn)}_2$ , along with 1-benzylisoquinoline,  $17^{\text{Ar}}$ , through a process of hydrogen transfer.<sup>[54]</sup> The same product was formed from  $5_{fc}^M\text{-THF}$  (Scheme 9). That reaction was general and the products were also characterized for  $16_{fc}^{\text{Lu}}\text{-(iqn)}_2$  and  $16_{py}^M\text{-(iqn)}_2$  ( $M = \text{Y}, \text{Lu}$ ), which were obtained from  $5_{Ad}^{\text{Lu}}\text{-(iqn)}_2$  and  $5_{py}^M\text{-(iqn)}_2$  ( $M = \text{Y}, \text{Lu}$ ), respectively (Scheme 9).<sup>[55,57]</sup>

The compounds  $16_{fc}^{\text{Lu}}\text{-(iqn)}_2$  and  $16_{py}^{\text{Y}}\text{-(iqn)}_2$  were characterized by single-crystal X-ray diffraction (Figure 15), which confirmed that two

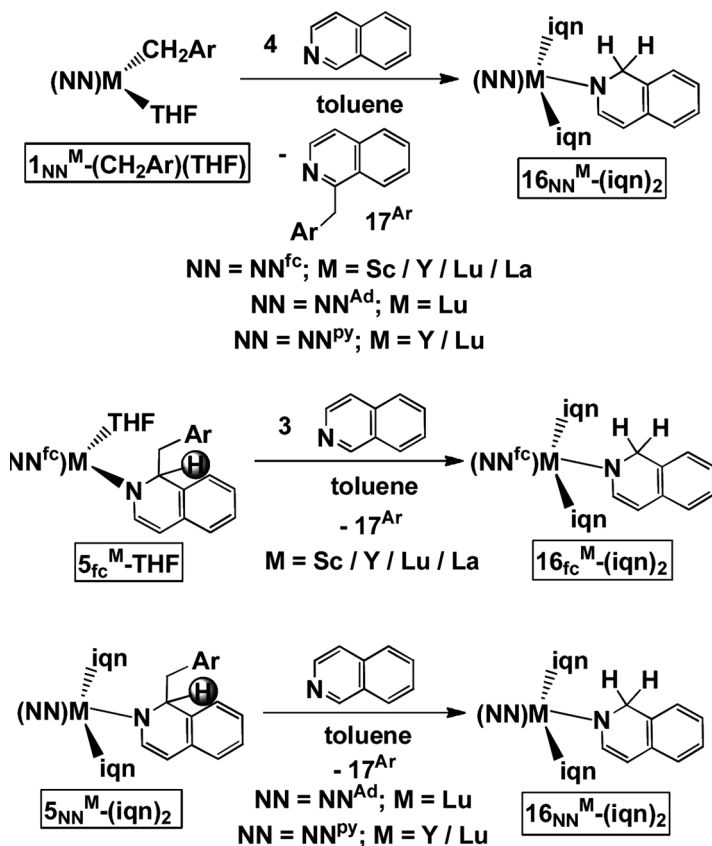


**Figure 14.** ORTEP representation (thermal ellipsoids at 50% probability) of  $15^Y_{fc}\text{-py}^{\text{Ph}}$  (left) and  $15^{\text{Lu}}_{fc}\text{-py}^{\text{Ph}}$  (right); hydrogen atoms were removed for clarity. (Figure appears in color online.)

isoquinoline ligands were coordinated to the metal centers instead of one, as found in  $5^Y_{fc}\text{-iqn}^{\text{Me}}$ . It is likely that less steric crowding is present in  $16^{\text{Lu}}_{fc}\text{-(iqn)}_2$  and  $16^Y_{py}\text{-(iqn)}_2$  because of the absence of the benzyl group in the proximity of the metal center.



It is interesting to note that a pyridine product reminiscent of  $16^Y_{fc}\text{-(iqn)}_2$  could be isolated ( $16'_{fc}\text{-(py)}_2$ , Eq. 11), although the reaction of the benzyl complexes  $1^M_{NN}\text{-(CH}_2\text{Ar)(THF)}$  with pyridine usually gives mixtures, from which individual compounds could not be separated. The complex  $16^Y_{fc}\text{-(py)}_2$  is the product of a hydrogen migration to the 4-position, as identified by X-ray crystallography (Figure 16), instead of to the 2-position, as was the case for isoquinoline. The characterization of  $16^Y_{fc}\text{-(py)}_2$  by other methods was not possible because it could not be purified when its synthesis was attempted ulteriorly. Computational studies revealed that both the alkyl and hydrogen-transfer

Scheme 9. Hydrogen transfer in  $5_{\text{NN}}^{\text{M}}$  complexes.

reactions had high activation barriers that were similar in value in the case of pyridine. Furthermore, the product of the hydrogen-transfer reaction was not as stabilized with respect to the starting material as in the case of isoquinoline. All those findings explain why the reaction with pyridine leads to complicated mixtures of products.

The hydrogen transfer from  $5_{\text{fc}}^{\text{M}}\text{-THF}$  also occurred to unsaturated substrates with polar double bonds, such as ketones and azobenzene, but it did not take place when 2-butyne, diphenylacetylene, and ethylene were employed. During the study of the latter reactions, it was found that the self-transformation of  $5_{\text{fc}}^{\text{M}}\text{-THF}$  to  $16_{\text{fc}}^{\text{M}}\text{-(THF)}_2$  and  $18_{\text{fc}}^{\text{M}}$  occurred (Eq. 12).<sup>[54]</sup>

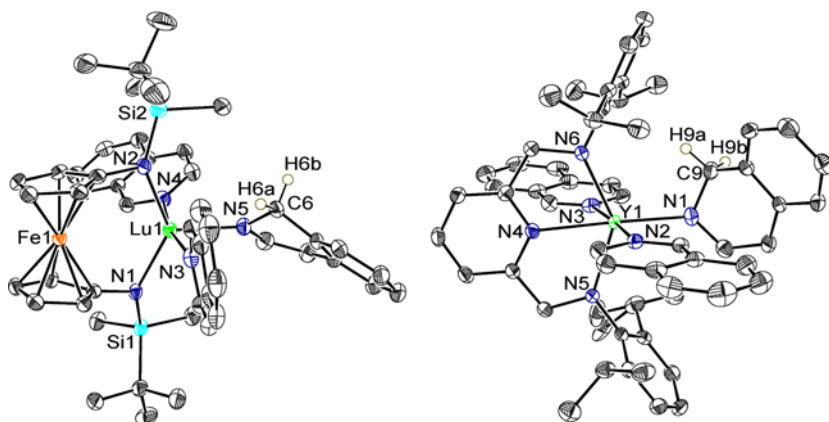


Figure 15. ORTEP representations (thermal ellipsoids at 50% probability) of  $16^{\text{Lu}}\text{-(iqn)}_2$  (left) and  $16^{\text{Y}}\text{-(iqn)}_2$  (right); irrelevant hydrogen atoms were removed for clarity. (Figure appears in color online.)

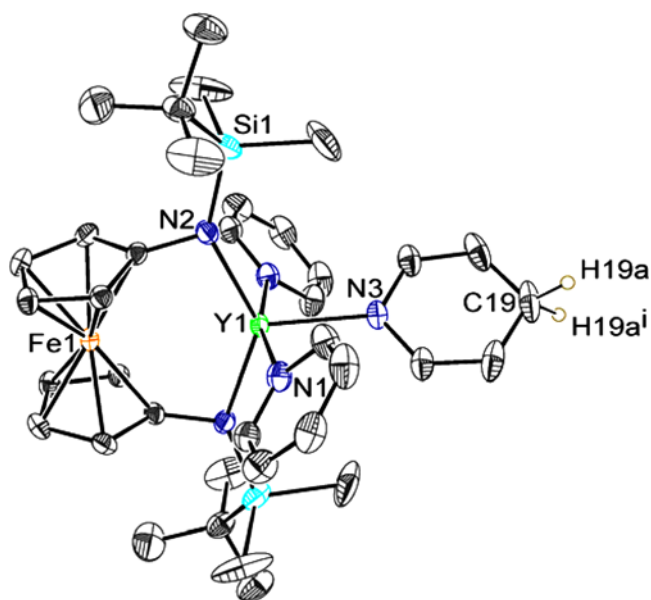
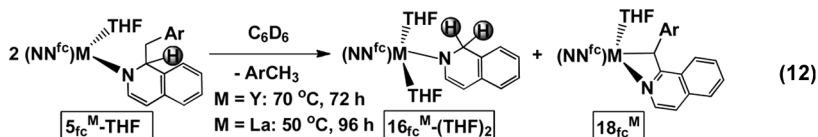
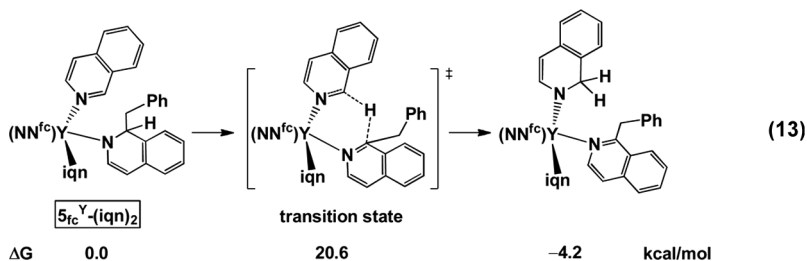


Figure 16. ORTEP representation (thermal ellipsoids at 35% probability) of  $16^{\text{Y}}\text{-(py)}_2$ ; irrelevant hydrogen atoms were removed for clarity. (Figure appears in color online.)



The reaction in Eq. 11 is somewhat similar to that reported by Cronin et al. for phenanthridinium salts:<sup>[115]</sup> in the presence of amines, the phenanthridinium salt was dearomatized and a product corresponding to  $5_{fc}^M\text{-THF}$  was formed. In the presence of a base, the dearomatized phenanthridinium transferred one proton to a molecule of the initial phenanthridinium salt, leading to the formation of a product corresponding to  $16_{fc}^M\text{-(THF)}_2$ , and underwent rearomatization, giving a product corresponding to  $18_{fc}^M$ .



A mechanism for the transformation of  $5_{fc}^M\text{-THF}$  to  $16_{fc}^M\text{-(iqn)}_2$  was proposed.<sup>[54]</sup> DFT calculations suggested that a direct transfer of a hydrogen atom between two isoquinoline ligands was the most plausible pathway (Eq. 13) and that the hydrogen atom migrated as a proton and not as a hydride. The results suggested that the activation barriers in the dearomatization of heterocycles was correlated with the lost versus gained aromatic stabilization energy.<sup>[54]</sup> That pathway was favored over  $\beta$ -hydride elimination.<sup>[54]</sup> Both types of mechanisms have been proposed to explain the Meerwein-Ponndorf-Verley reduction of ketones by various metal alkoxides,<sup>[116]</sup> a reaction similar to the transformation of  $5_{fc}^M\text{-THF}$  to  $16_{fc}^M\text{-(iqn)}_2$ .

#### 4. CONCLUSIONS

The present review discussed the chemistry of metal complexes supported by two types of chelating ferrocene ligands: (1) Schiff base and (2) diamide. The metals of interest were yttrium and cerium for the first class and group 3 metals (scandium, yttrium, lutetium, and lanthanum) for the latter.

Two series of Schiff base metal complexes were discussed. The two ancillary ligands differed by the type of the N=X functionality that they incorporated: one ligand was based on imine, whereas the other was based on an iminophosphorane group. The resulting cerium(IV) bis (alkoxide) complexes were characterized in order to determine whether the presence of the strongly oxidizing cerium(IV) would give rise to non-innocent redox behavior in the supporting ligands. For comparison, the corresponding cerium(III) and yttrium(III) alkoxide complexes were also synthesized. All the metal complexes were characterized by cyclic voltammetry and  $^1\text{H}$  NMR, Mössbauer, X-ray absorption near-edge structure (XANES), and absorption spectroscopies. The experimental data indicated that iron remained in the +2 oxidation state and that cerium(IV) did not engage any part of the ancillary ligand in redox behavior.

1,1'-Ferrocene-diamide complexes of group 3 metals showed a diverse array of reactivity with aromatic N-heterocycles. Those reactions were investigated and a substrate-dependent behavior was observed. For example, 1-methylimidazole was cleaved by all the metal complexes studied. With pyridines, subtle differences in behavior were identified: C-H activation and C-C coupling were operative for ortho-substituted pyridines, while alkyl transfer was manifested for isoquinoline and chelating pyridines. The product of those reactions underwent further transformations. For example, migratory insertions took place between pyridyl complexes and unsaturated substrates. On the other hand, the products of the C-C coupling reactions were found to undergo two types of hydrogen transfers: (1) isomerization within the same ring to give extended-conjugated structures; and (2) H $\cdot$  abstraction to give radical-anionic bipyridyl complexes. The products of alkyl-transfer reactions also underwent a subsequent hydrogen-transfer reaction, which occurred between two different heterocycles.

The comparison between the ferrocene and pyridine-diamide benzyl complexes showed that similar reactions were observed with 1-methylimidazole, 2-picoline, and isoquinoline. It is important to note, however, that other types of reactions and a larger substrate scope were identified for the ferrocene- than for the pyridine-based complexes.

Although some of the reactions observed with the ferrocene-diamide group 3 metal benzyl complexes have been previously reported for other classes of compounds, those examples were isolated and, in some cases, the reactions were not straightforward. In this light, the ferrocene diamides represent a versatile ligand framework. That finding was significant

because the analysis of different reactivity behaviors with one class of complexes allowed comparisons to be made and factors leading to individual reactions to be rationalized. It is possible that the privileged status of these organometallic ancillary ligands is a consequence of iron's ability to accommodate changes in the electronic density at the metal center more readily than classical supporting ligands.

## ACKNOWLEDGMENTS

The efforts of present and former members of the Diaconescu laboratory were crucial in making this project possible. Their names, together with those of valuable collaborators, appear in the references from which this account draws. The research summarized herein has been funded by the UCLA, UC Energy Institute, Sloan Foundation, and NSF (Grant CHE-0847735).

## REFERENCES

1. Kealy, T. J. and P. L. Pauson. 1951. A new type of organo-iron compound. *Nature*, **168**: 1039–1040.
2. Miller, S. A., J. A. Tebboth, and J. F. Tremaine. 1952. Dicyclopentadienyl iron. *J. Chem. Soc.*, **XX**: 632–635.
3. Wilkinson, G., M. Rosenblum, M. C. Whiting, and R. B. Woodward. 1952. The structure of iron bis-cyclopentadienyl. *J. Am. Chem. Soc.*, **74**(8): 2125–2126.
4. Fischer, E. O. and W. Pfab. 1952. Cyclopentadien-Metallkomplexe, ein neuer typ metallorganischer Verbindungen. *Z. Naturforsch. B*, **7**: 377–379.
5. Eiland, P. F. and R. Pepinsky. 1952. X-ray examination of iron biscyclopentadienyl. *J. Am. Chem. Soc.*, 1952, **74**(19): 4971–4971.
6. Nobel Foundation. 1973. The 1973 Nobel Prize in Chemistry. [http://nobelprize.org/nobel\\_prizes/chemistry/laureates/1973/press.html](http://nobelprize.org/nobel_prizes/chemistry/laureates/1973/press.html)
7. Štěpnička, P. 2008. *Ferrocenes: Ligands, Materials and Biomolecules*, West Sussex, UK: Wiley.
8. Togni, A. and T. Hayashi. 1995. *Ferrocenes: Homogeneous Catalysis, Organic Synthesis, Materials Science*, Weinheim, Germany: VCH Publishers.
9. Connelly, N. G. and W. E. Geiger. 1996. Chemical redox agents for organometallic chemistry. *Chem. Rev.*, **96**(2): 877–910.
10. Stubbe, J. and W. A. van der Donk. 1998. Protein radicals in enzyme catalysis. *Chem. Rev.*, **98**(2): 705–762.
11. Jazdzewski, B. A. and W. B. Tolman. 2000. Understanding the copper-phenoxyl radical array in galactose oxidase: contributions from synthetic modeling studies. *Coord. Chem. Rev.*, **200–202**: 633–685.

12. Fuhrhop, J. H. 1974. The reactivity of the porphyrin ligand. *Angew. Chem. Int. Ed.*, **13**(5): 321–335.
13. Chaudhuri, P. and K. Wieghardt. 2001. Phenoxyl radical complexes. *Prog. Inorg. Chem.*, **50**: 151–216.
14. Grützmacher, H. 2008. Cooperating ligands in catalysis. *Angew. Chem. Int. Ed.*, **47**(10): 1814–1818.
15. Marr, G. and T. Hunt. 1969. Unsymmetrically disubstituted ferrocenes. Part VIII. Synthesis and reactivity of some 2-substituted ferrocenylphosphines. *J. Chem. Soc. C*, 1070–1072.
16. Bishop, J. J., A. Davison, M. L. Katcher, D. W. Lichtenberg, R. E. Merrill, and J. C. Smart. 1971. Symmetrically disubstituted ferrocenes: I. The synthesis of potential bidentate ligands. *J. Organomet. Chem.*, **27**(2): 241–249.
17. Gibson, V. C. and S. K. Spitzmesser. 2003. Advances in non-metallocene olefin polymerization catalysis. *Chem. Rev.*, **103**(1): 283–315.
18. Piers, W. E. and D. J. H. Emslie. 2002. Non-cyclopentadienyl ancillaries in organogroup 3 metal chemistry: a fine balance in ligand design. *Coord. Chem. Rev.*, **233–234**: 131–155.
19. Siemeling, U. and T.-C. Auch. 2005. 1,1'-Di(heteroatom)-functionalised ferrocenes as [N,N], [O,O] and [S,S] chelate ligands in transition metal chemistry. *Chem. Soc. Rev.*, **34**(7): 584.
20. Broderick, E. M. and P. L. Diaconescu. 2009. Cerium(IV) catalysts for the ring-opening polymerization of lactide. *Inorg. Chem.*, **48**: 4701–4706.
21. Broderick, E. M., P. Thuy-Boun, N. Guo, C. Vogel, J. Sutter, J. T. Miller, K. Meyer, and P. L. Diaconescu. 2010. Synthesis and characterization of cerium and yttrium alkoxide complexes supported by ferrocene-based chelating ligands. submitted.
22. Shafir, A., D. Fiedler, and J. Arnold. 2002. Formation of 1: 1 complexes of ferrocene-containing salen ligands with Mg, Ti and Zr. *J. Chem. Soc., Dalton Trans.*, **4**: 555–560.
23. Holm, R. H., J. G. W. Everett, and A. Chakravorty. 1966. Metal complexes of Schiff bases and beta-Ketoamines. In *Prog. Inorg. Chem.*, Cotton, F. A. (ed.), **7**: 83–214.
24. Kapturkiewicz, A. and B. Behr. 1983. Voltammetric studies of Co(salen) and Ni(salen) in nonaqueous solvents at Pt electrode. *Inorg. Chim. Acta*, **69**: 247–251.
25. Zanello, P. and A. Cinquantini. 1985. Electrochemical behaviour of a series of *N,N'*-1,2-Phenylenebis(salicylideneiminato) transition metal complexes. *Trans. Met. Chem.*, **10**(10): 370–374.
26. Roy, N., S. Sproules, T. Weyhermüller, and K. Wieghardt. 2009. Trivalent iron and ruthenium complexes with a redox noninnocent (2-Mercapto phenylimino)-methyl-4,6-di-tert-butylphenolate(2-) ligand. *Inorg. Chem.*, **48**(8): 3783–3791.



27. De Castro, B. and C. Freire. 1990. EPR and electrochemical study of nickel(III) complexes of bis(3,5-dichlorosalicylaldehyde) o-phenylenediimine. Evidence for adduct formation with pyridines. *Inorg. Chem.*, **29**(25): 5113–5119.
28. Vilas-Boas, M., C. Freire, B. de Castro, P. A. Christensen, and A. R. Hillman. 1997. New insights into the structure and properties of electroactive polymer films derived from [Ni(salen)]. *Inorg. Chem.*, **36**(22): 4919–4929.
29. de Castro, B., C. Freire, and E. Pereira. 1994. Decomposition of chemically and electrochemically generated nickel(III) complexes with N<sub>2</sub>O<sub>2</sub> Schiff-base ligands. *J. Chem. Soc., Dalton Trans.*, 571–576.
30. Freire, C. and B. de Castro. 1998. Spectroscopic characterisation of electro-generated nickel(III) species. Complexes with N<sub>2</sub>O<sub>2</sub> Schiff-base ligands derived from salicylaldehyde. *J. Chem. Soc., Dalton Trans.*, 1491–1498.
31. de C.T. Carrondo, M. A. A. F., B. de Castro, A. M. Coelho, D. Domingues, C. Freire, and J. Morais. 1993. Electrochemical and structural studies of nickel(II) complexes with N<sub>2</sub>O<sub>2</sub> Schiff base ligands derived from 2-hydroxy-1-naphthaldehyde. Molecular structure of N,N'-2,3-dimethylbutane-2,3-diyl-bis(2-hydroxy-1-naphthylideneimine) nickel(II). *Inorg. Chim. Acta*, **205**(2): 157–166.
32. Goldsby, K. A., J. K. Blaho, and L. A. Hoferkamp. 1989. Oxidation of nickel(II) bis(salicylaldehyde) complexes: Solvent control of the ultimate redox site. *Polyhedron*, **8**(1): 113–115.
33. Azevedo, F., M. A. A. F. de C.T. Carrondo, B. de Castro, M. Convery, D. Domingues, C. Freire, M. T. Duarte, K. Nielsen, and I. C. Santos. 1994. Electrochemical and structural studies of nickel(II) complexes with N<sub>2</sub>O<sub>2</sub> Schiff base ligands 2. Crystal and molecular structure of N,N'-1,2-ethane-1,2-diyl-bis(2-hydroxyacetophenonylideneimine)nickel(II), N, N'-1,2-cis cyclohexane-1,2-diyl-bis(2-hydroxyacetophenonylideneimine)- nickel(II) and N,N'-1,2-benzene-1,2-diyl-bis(3,5-dichlorosalicylideneimine)nickel(II). *Inorg. Chim. Acta*, **219**(1–2): 43–54.
34. Shimazaki, Y., F. Tani, K. I. Fukui, Y. Naruta, and O. Yamauchi. 2003. One-electron oxidized nickel(II)-(disalicylidene)diamine complex: Temperature-dependent tautomerism between Ni(III)-phenolate and Ni(II)-phenoxy radical states. *J. Am. Chem. Soc.*, **125**(35): 10512–10513.
35. Shimazaki, Y., T. Yajima, F. Tani, S. Karasawa, K. Fukui, Y. Naruta, and O. Yamauchi. 2007. Syntheses and electronic structures of one-electron-oxidized Group 10 Metal(II)-(Disalicylidene)diamine complexes (metal = Ni, Pd, Pt). *J. Am. Chem. Soc.*, **129**(9): 2559–2568.
36. Orio, M., O. Jarjays, H. Kanso, C. Philouze, F. Neese, and F. Thomas. 2010. X-ray structures of copper(II) and nickel(II) radical salen complexes: The preference of galactose oxidase for copper(II). *Angew. Chem. Int. Ed.*, **49**(29): 4989–4992.

37. Yamashita, M., Y. Takemoto, E. Ihara, and H. Yasuda. 1996. Organolanthanide-initiated living polymerizations of  $\epsilon$ -Caprolactone,  $\delta$ -Valerolactone, and  $\beta$ -Propiolactone. *Macromolecules*, **29**: 1798.
38. Hodgson, L. M., A. J. P. White, and C. K. Williams. 2006. Yttrium(III) complex as a highly active catalyst for lactide polymerization. *J. Polym. Sci. A: Polym. Chem.*, **44**(22): 6646–6651.
39. Patel, D., S. T. Liddle, S. A. Mungur, M. Rodden, A. J. Blake, and P. L. Arnold. 2006. Bifunctional yttrium(III) and titanium(IV) NHC catalysts for lactide polymerisation. *Chem. Commun.*, **10**: 1124–1126.
40. Ma, H., T. P. Spaniol, and J. Okuda. 2008. Rare-earth metal complexes supported by 1, $\omega$ -dithiaalkanedyl-bridged Bis(phenolato) ligands: Synthesis, structure, and heteroselective ring-opening polymerization of rac-Lactide. *Inorg. Chem.*, **47**(8): 3328–3339.
41. Nomura, N., A. Taira, A. Nakase, T. Tomioka, and M. Okada. 2007. Ring-opening polymerization of lactones by rare-earth metal triflates and by their reusable system in ionic liquids. *Tetrahedron*, 2007, **63**(35): 8478–8484.
42. Shafir, A., M. P. Power, G. D. Whitener, and J. Arnold. 2001. Silylated 1,1'-diaminoferrocene: Ti and Zr complexes of a new chelating diamide ligand. *Organometallics*, **20**(7): 1365–1369.
43. Shafir, A. and J. Arnold. 2003. Zirconium complexes incorporating diaryldiamidoferrocene ligands: generation of cationic derivatives and polymerization activity towards ethylene and 1-hexene. *Inorg. Chim. Acta*, **345**: 216–220.
44. Shafir, A. and J. Arnold. 2003. Ferrocene-based olefin polymerization catalysts: activation, structure, and intermediates. *Organometallics*, **22**(3): 567–575.
45. Shafir, A. and J. Arnold. 2001. Stabilization of a cationic Ti center by a ferrocene moiety: A remarkably short Ti-Fe interaction in the diamide  $\{[(\eta^5\text{-C}_5\text{H}_4\text{NSiMe}_3)_2\text{Fe}]\text{TiCl}\}_2^{2+}$ . *J. Am. Chem. Soc.*, **123**(37): 9212–9213.
46. Seyferth, D., B. W. Hames, T. G. Rucker, M. Cowie, and R. S. Dickson. 1983. A novel palladium complex with iron-palladium dative bonding derived from 1,2,3-trithia[3]ferrocenophane( $\text{Ph}_3\text{P}$ )PdFe( $\text{SC}_5\text{H}_4$ ) $_2$ .0.5C $_6$ H $_5$ CH $_3$ . *Organometallics*, **2**: 472–474.
47. Ramos, A., E. Otten, and D. W. Stephan. 2009. Stabilizing Zr and Ti cations by interaction with a ferrocenyl fragment. *J. Am. Chem. Soc.*, **131**: 15610–15611.
48. Wrackmeyer, B., E. V. Klimkina, and W. Milius. 2008. Five- and four-coordinate 1,3-Diaza-2-ytttria- and 1,3-Diaza-2-scandia-[3]ferrocenophanes. *Eur. J. Inorg. Chem.*, 3340–3347.
49. Eppinger, J., K. R. Nikolaides, M. Zhang-Prese, F. A. Riederer, G. W. Rabe, and A. L. Rheingold. 2008. Alkyl complexes of rare-earth metal centers supported by chelating 1,1'-diamidoferrocene ligands: Synthesis,

- structure, and application in methacrylate polymerization. *Organometallics*, **27**(4): 736–740.
50. Diaconescu, P. L. 2010. Reactions of aromatic n-heterocycles with  $d^0f^n$ -metal alkyl complexes supported by chelating diamide ligands. *Acc. Chem. Res.*, **43**(10): 1352–1363.
51. Carver, C. T., M. J. Monreal, and P. L. Diaconescu. 2008. Scandium alkyl complexes supported by a ferrocene diamide ligand. *Organometallics*, **27**: 363–370.
52. Carver, C. T. and P. L. Diaconescu. 2008. Ring-opening reactions of aromatic N-heterocycles by scandium and yttrium alkyl complexes. *J. Am. Chem. Soc.*, **130**: 7558–7559.
53. Carver, C. T., D. Benitez, K. L. Miller, B. N. Williams, E. Tkatchouk, W. A. Goddard, and P. L. Diaconescu. 2009. Reactions of Group III biheterocyclic complexes. *J. Am. Chem. Soc.*, **131**: 10269–10278.
54. Miller, K. L., B. N. Williams, D. Benitez, C. T. Carver, K. R. Ogilby, E. Tkatchouk, W. A. Goddard, and P. L. Diaconescu. 2010. Dearomatization reactions of N-heterocycles mediated by Group 3 complexes. *J. Am. Chem. Soc.*, **132**: 342–355.
55. Jie, S. and P. L. Diaconescu. 2010. Reactions of aromatic N-heterocycles with yttrium and lutetium benzyl complexes supported by a pyridine-diamide ligand. *Organometallics*, **29**(5): 1222–1230.
56. Cordero, B., V. Gomez, A. E. Platero-Prats, M. Reves, J. Echeverria, E. Cremades, F. Barragan, and S. Alvarez. 2008. Covalent radii revisited. *Dalton Trans.*, **21**: 2832–2838.
57. Wong, A. W., K. L. Miller, and P. L. Diaconescu. 2010. Reactions of aromatic N-heterocycles with a lutetium benzyl complex supported by a ferrocene-diamide ligand. *Dalton Trans.*, **39**(29): 6726–6731.
58. Tsuruta, H., T. Imamoto, and K. Yamaguchi. 1999. Evaluation of the relative Lewis acidities of lanthanoid(III) compounds by tandem mass spectrometry. *Chem. Commun.*, 1703–1704.
59. Jordan, R. F. and A. S. Guram. 1990. Scope and regiochemistry of ligand carbon-hydrogen activation reactions of  $Cp_2Zr(CH_3)(THF)^+$ . *Organometallics*, **9**(7): 2116–2123.
60. Chinchilla, R., C. Najera, and M. Yus. 2004. Metalated heterocycles and their applications in synthetic organic chemistry. *Chem. Rev.*, **104**: 2667–2722.
61. Watson, P. L. 1983. Methane exchange reactions of lanthanide and early-transition-metal methyl complexes. *J. Am. Chem. Soc.*, **105**(21): 6491–6493.
62. Thompson, M. E., S. M. Baxter, A. R. Bulls, B. J. Burger, M. C. Nolan, B. D. Santarsiero, W. P. Schaefer, and J. E. Bercaw. 1987.  $\sigma$ -Bond metathesis for carbon-hydrogen bonds of hydrocarbons and Sc-R (R = H, alkyl, aryl)

- bonds of permethylscandocene derivatives. Evidence for noninvolvement of the  $\pi$  system in electrophilic activation of aromatic and vinylic C–H bonds. *J. Am. Chem. Soc.*, **109**(1): 203–219.
63. Bercaw, J. E. 1990. Carbon-hydrogen and carbon-carbon bond activation with highly electrophilic transition metal complexes. *Pure Appl. Chem.*, **62**(6): 1151–1154.
64. Carver, C. T., B. N. Williams, K. R. Ogilby, and P. L. Diaconescu. 2010. Coupling of aromatic N-heterocycles mediated by Group 3 complexes. *Organometallics*, **29**(4): 835–846.
65. Carver, C. T. and P. L. Diaconescu. 2009. Insertion reactions of scandium pyridyl complexes supported by a ferrocene diamide ligand. *J. Alloys Compd.*, **488**(2): 518–523.
66. Duchateau, R., E. A. C. Brussee, A. Meetsma, and J. H. Teuben. 1997. Synthesis and reactivity of Bis(alkoxysilylamido)yttrium  $\eta^2$ -Pyridyl and  $\eta^2$ - $\alpha$ -Picolyl compounds. *Organometallics*, **16**: 5506–5516.
67. Kiplinger, J. L., B. L. Scott, E. J. Schelter, and J. A. Pool Davis Tournear. 2007.  $sp^3$  versus  $sp^2$  C–H bond activation chemistry of 2-picoline by Th(IV) and U(IV) metallocene complexes. *J. Alloys Compd.*, **444–445**: 477–482.
68. Jordan, R. F. and A. S. Guram. 1990. Scope and regiochemistry of ligand carbon-hydrogen activation reactions of  $Cp_2Zr(CH_3)(THF)^+$ . *Organometallics*, **9**: 2116–2123.
69. Jantunen, K. C., B. L. Scott, P. J. Hay, J. C. Gordon, and J. L. Kiplinger. 2006. Dearomatization and functionalization of terpyridine by lutetium(III) alkyl complexes. *J. Am. Chem. Soc.*, **128**: 6322–6323.
70. D'Souza, D. M. and T. J. J. Muller. 2007. Multi-component syntheses of heterocycles by transition-metal catalysis. *Chem. Soc. Rev.*, **36**(7): 1095–1108.
71. Zeni, G. and R. C. Larock. 2004. Synthesis of heterocycles via palladium  $\pi$ -olefin and  $\pi$ -alkyne chemistry. *Chem. Rev.*, **104**(5): 2285–2310.
72. Nakamura, I. and Y. Yamamoto. 2004. Transition-metal-catalyzed reactions in heterocyclic synthesis. *Chem. Rev.*, **104**(5): 2127–2198.
73. Balme, G., E. Bossharth, and N. Monteiro. 2003. Pd-assisted multicomponent synthesis of heterocycles. *Eur. J. Org. Chem.*, **21**: 4101–4111.
74. Davies, H. M. L. and S. J. Hedley. 2007. Intermolecular reactions of electron-rich heterocycles with copper and rhodium carbenoids. *Chem. Soc. Rev.*, **36**(7): 1109–1119.
75. Chemler, S. R. and P. H. Fuller. 2007. Heterocycle synthesis by copper facilitated addition of heteroatoms to alkenes, alkynes and arenes. *Chem. Soc. Rev.*, **36**(7): 1153–1160.
76. Mihovilovic, M. D. and P. Stanetty. 2007. Metal-assisted multicomponent reactions involving carbon monoxide - towards heterocycle synthesis. *Angew. Chem. Int. Ed.*, **46**(20): 3612–3615.

77. Padwa, A. and S. K. Bur. 2007. The domino way to heterocycles. *Tetrahedron*, **63**(25): 5341–5378.
78. Jordan, R. F., D. F. Taylor, and N. C. Baenziger. 1990. Synthesis and insertion chemistry of cationic zirconium(IV) pyridyl complexes. Productive  $\sigma$ -bond metathesis. *Organometallics*, **9**(5): 1546–1557.
79. Guram, A. S. and R. F. Jordan. 1991. Alkene and alkyne insertion reactions of cationic  $\text{Cp}_2\text{Zr}(\eta^2\text{-pyridyl})(\text{L})^+$  complexes. Zirconium-mediated functionalization of pyridines. *Organometallics*, **10**(10): 3470–3479.
80. Jordan, R. F. 1991. Chemistry of cationic dicyclopentadienyl group-4 metal alkyl complexes. *Adv. Organomet. Chem.*, **32**: 325–387.
81. Lewis, J. C., R. G. Bergman, and J. A. Ellman. 2007. Rh(I)-catalyzed alkylation of quinolines and pyridines via C–H bond activation. *J. Am. Chem. Soc.*, **129**(17): 5332–5333.
82. Tan, K. L., R. G. Bergman, and J. A. Ellman. 2001. Annulation of alkenyl-substituted heterocycles via rhodium-catalyzed intramolecular C–H activated coupling reactions. *J. Am. Chem. Soc.*, **123**(11): 2685–2686.
83. Tan, K. L., R. G. Bergman, and J. A. Ellman. 2002. Intermolecular coupling of isomerizable alkenes to heterocycles via rhodium-catalyzed C–H bond activation. *J. Am. Chem. Soc.*, **124**(47): 13964–13965.
84. Tan, K. L., S. Park, J. A. Ellman, and R. G. Bergman. 2004. Intermolecular coupling of alkenes to heterocycles via C–H bond activation. *J. Org. Chem.*, **69**(21): 7329–7335.
85. Wiedemann, S. H., R. G. Bergman, and J. A. Ellman. 2004. Rhodium-catalyzed direct C–H addition of 4,4-Dimethyl-2-oxazoline to alkenes. *Org. Lett.*, **6**(10): 1685–1687.
86. Wiedemann, S. H., J. A. Ellman, and R. G. Bergman. 2006. Rhodium-catalyzed direct C–H addition of 3,4-dihydroquinazolines to alkenes and their use in the total synthesis of vasicoline. *J. Org. Chem.*, **71**(5): 1969–1976.
87. Kakiuchi, F. and S. Murai. 2002. Catalytic C–H/olefin coupling. *Acc. Chem. Res.*, **35**(10): 826–834.
88. Fujii, N. K. F., N. Chatani, and S. Murai. 1996. Transition metal-catalyzed intramolecular C–H/olefin coupling. *Chem. Lett.*, 939–940.
89. Fujii, N. K. F., A. Yamada, N. Chatani, and S. Murai. 1997. Asymmetric intramolecular C–H/olefin coupling: asymmetric cyclization reactions of 1,5-dienes catalyzed by rhodium complexes. *Chem. Lett.*, 425–426.
90. Fujii, N. K. F., A. Yamada, N. Chatani, and S. Murai. 1998. Transition metal-catalyzed intramolecular cyclization of 1,5- and 1,6-dienes via direct cleavage and addition of the carbon-hydrogen bond. *Bull. Chem. Soc. Jpn.*, **71**: 285–298.
91. Zhang, Z., X. Wang, and R. A. Widenhoefer. 2006. Platinum(II)-catalyzed intermolecular hydroarylation of unactivated alkenes with indoles. *Chem. Commun.*, **35**: 3717–3719.

92. Liu, C., X. Han, X. Wang, and R. A. Widenhoefer. 2004. Platinum-catalyzed intramolecular alkylation of indoles with unactivated olefins. *J. Am. Chem. Soc.*, **126**(12): 3700–3701.
93. Han, X. and R. A. Widenhoefer. 2006. Platinum-catalyzed intramolecular asymmetric hydroarylation of unactivated alkenes with indoles. *Org. Lett.*, **8**(17): 3801–3804.
94. Jordan, R. F. and D. F. Taylor. 1989. Zirconium-catalyzed coupling of propene and  $\alpha$ -picoline. *J. Am. Chem. Soc.*, **111**(2): 778–779.
95. Guram, A. S., R. F. Jordan, and D. F. Taylor. 1991. Insertion chemistry of  $\text{Cp}_2\text{Zr}(\eta^2\text{-C}_5\text{H}_4\text{N-CH}_2\{6\text{-Me-pyrid-2-yl}\})^+$ : facile zirconium-mediated functionalization of methyl carbon-hydrogen bonds of 2,6-lutidine. *J. Am. Chem. Soc.*, **113**(5): 1833–1835.
96. Deelman, B.-J., W. M. Stevels, J. H. Teuben, M. T. Lakin, and A. L. Spek. 1994. Insertion chemistry of yttrium complex  $\text{Cp}^*\text{Y}(2\text{-pyridyl})$  and molecular structure of an unexpected CO insertion product  $(\text{Cp}^*\text{Y})_2(\mu\text{-}\eta^2\text{:}\eta^2\text{-OC}(\text{NC}_5\text{H}_4)_2)$ . *Organometallics*, **13**(10): 3881–3891.
97. Abrams, M. B., J. C. Yoder, C. Loeber, M. W. Day, and J. E. Bercaw. 1999. Fluxional  $\eta^3$ -Allyl derivatives of ansa-scandocenes and an ansa-yttrocene. measurements of the barriers for the  $\eta^3$  to  $\eta^1$  process as an indicator of olefin binding energy to  $d^0$  metallocenes. *Organometallics*, **18**(8): 1389–1401.
98. Monreal, M. J. and P. L. Diaconescu. 2010. Reversible C–C coupling in a uranium biheterocyclic complex. *J. Am. Chem. Soc.*, **132**(22): 7676–7683.
99. Miller, K. L., C. T. Carver, B. N. Williams, and P. L. Diaconescu. 2010. Reactions of imidazoles with electrophilic metal alkyl complexes. *Organometallics*, **29**(10): 2272–2281.
100. Allen, K. D., M. A. Bruck, S. D. Gray, R. P. Kingsborough, D. P. Smith, K. J. Weller, and D. E. Wigley. 1995. Quinoline binding mode as a function of oxidation state in aryloxy-supported tantalum complexes: Models for hydrodenitrogenation catalysis. *Polyhedron*, **14**(22): 3315–3333.
101. Kleckley, T. S., J. L. Bennett, P. T. Wolczanski, and E. B. Lobkovsky. 1997. Pyridine C=N bond cleavage mediated by  $(\text{silox})_3\text{Nb}$  ( $\text{silox} = t\text{-Bu}_3\text{SiO}$ ). *J. Am. Chem. Soc.*, **119**(1): 247–248.
102. Neithamer, D. R., L. Parkanyi, J. F. Mitchell, and P. T. Wolczanski. 1988.  $\eta^2$ -(N,C)-pyridine and  $\mu\text{-}\eta^2(1,2)\text{:}\eta^2(4,5)$ -benzene complexes of  $(\text{silox})_3\text{Ta}$  ( $\text{silox} = t\text{-Bu}_3\text{SiO}$ ). *J. Am. Chem. Soc.*, **110**(13): 4421–4423.
103. Fout, A. R., B. C. Bailey, J. Tomaszewski, and D. J. Mindiola. 2007. Cyclic denitrogenation of N-heterocycles applying a homogeneous titanium reagent. *J. Am. Chem. Soc.*, **129**(42): 12640–12641.
104. Bailey, B. C., H. Fan, J. C. Huffman, M. H. Baik, and D. J. Mindiola. 2006. Room temperature ring-opening metathesis of pyridines by a transient TiC linkage. *J. Am. Chem. Soc.*, **128**(21): 6798–6799.

105. Huertos, M. A., J. Perez, and L. Riera. 2008. Pyridine ring opening at room temperature at a rhenium tricarbonyl bipyridine complex. *J. Am. Chem. Soc.*, **130**(17): 5662–5663.
106. Huertos, M. A., J. Pérez, L. Riera, and A. Menéndez-Velaázquez. 2008. From N-Alkylimidazole ligands at a rhenium center: ring opening or formation of NHC complexes. *J. Am. Chem. Soc.*, **130**(41): 13530–13531.
107. Sattler, A. and G. Parkin. 2010. Cleaving carbon-carbon bonds by inserting tungsten into unstrained aromatic rings. *Nature*, **463**: 523–526.
108. Monreal, M. J., S. Khan, and P. L. Diaconescu. 2009. Beyond C–H activation with uranium: A cascade of reactions mediated by a uranium dialkyl complex. *Angew. Chem. Int. Ed.*, **48**(44): 8352–8355.
109. Duhović, S., M. J. Monreal, and P. L. Diaconescu. 2010. Reactions of aromatic heterocycles with uranium alkyl complexes. *Inorg. Chem.*, **49**(15): 7165–7169.
110. Duhović, S., M. J. Monreal, and P. L. Diaconescu. 2010. Ring opening of aromatic heterocycles by uranium complexes. *J. Organomet. Chem.*, Pacificchem2010, DOI: 10.1016/j.jorganchem.2010.08.003.
111. Pool, J. A., B. L. Scott, and J. L. Kiplinger. 2005. Carbon-nitrogen bond cleavage in pyridine ring systems mediated by organometallic thorium(IV) complexes. *Chem. Commun.*, **20**: 2591–2593.
112. Arunachalampillai, A., P. Crewdson, I. Korobkov, and S. Gambarotta. 2006. Ring opening and C–O and C–N bond cleavage by transient reduced thorium species. *Organometallics*, **25**: 3856–3866.
113. Huang, W., C. T. Carver, and P. L. Diaconescu. 2010. Transmetallation reactions of a scandium complex supported by a ferrocene-diamide ligand. *Inorg. Chem.*, in press.
114. Williams, B. N., W. Huang, K. L. Miller, and P. L. Diaconescu. 2010. Group 3 metal complexes of radical-anionic 2,2'-bipyridyl ligands. *Inorg. Chem.*, in press.
115. Parenty, A. D. C., L. V. Smith, A. L. Pickering, D.-L. Long, and L. Cronin. 2004. General one-pot, three-step methodology leading to an extended class of n-heterocyclic cations: spontaneous nucleophilic addition, cyclization, and hydride loss. *J. Org. Chem.*, **69**: 5934–5946.
116. Cha, J. S. 2006. Recent developments in Meerwein-Ponndorf-Verley and related reactions for the reduction of organic functional groups using aluminum, boron, and other metal reagents: a review. *Org. Proc. Res. Dev.*, **10**: 1032–1053.